

Damping of spin waves in a two-dimensional Heisenberg antiferromagnet at low temperatures

Stéphane Tyč* and Bertrand I. Halperin

Jefferson Laboratory of Physics, Harvard University, Cambridge, Massachusetts 02138

(Received 24 October 1989)

The Dyson-Maleev formalism is used to calculate the damping of spin waves in the two-dimensional Heisenberg antiferromagnet at asymptotically low temperatures and long wavelengths, both in the quantum and in the classical case. The calculations are done self-consistently. Various regimes are found for the decay rate depending on the relative size of the reduced temperature τ and the dimensionless wave vector ka . In all cases, the decay rate is found to be much smaller than the frequency of the excitations, leading to well-defined spin waves, provided that $k\xi \gg 1$, where the correlation length ξ is of order $\exp(\text{const}/\tau)$. At low but finite temperatures, we take into account fluctuation renormalizations which tend to increase the damping. The result of simulations on the classical lattice rotor model are presented and compared with the calculations. The agreement is qualitatively good. The simulations are also used to test the scaling form for the decay rate in the regime $k\xi \sim 1$, which is outside the limit of validity of our direct spin-wave calculations.

I. INTRODUCTION

Since the discovery of high-temperature superconductivity, the two-dimensional (2D) quantum Heisenberg antiferromagnet (QHAF) has been the focus of much attention. Some of the new superconductors (e.g., La_2CuO_4) display strong antiferromagnetic ordering in their insulating (stoichiometric) phase which can be understood in terms of a QHAF model.¹ Inelastic neutron-scattering experiments, which have been used to probe the antiferromagnetic ordering of La_2CuO_4 , give a measure of the order-parameter dynamic-correlation function $S(k, \omega)$, where the order parameter is the staggered magnetization.²⁻⁴ Based on the results of renormalization-group calculations, hydrodynamics, and scaling arguments, Chakravarty, Halperin, and Nelson¹ (CHN) have proposed a scaling form for the dynamic-correlation function $S(k, \omega)$ for the 2D QHAF, which exhibits well-defined spin-wave peaks at low temperatures and long wavelengths provided that the wave vector k is large compared to the inverse correlation length ξ^{-1} . CHN used hydrodynamics to predict the spin-wave frequency $\omega(k)$, but they recognized that hydrodynamics could not be used to evaluate the spin-wave damping Γ_k . Indeed, in 2D, the most important damping mechanism comes from long-wavelength spin-wave scattering, rather than short-wavelength fluctuations. More recently, Tyč, Halperin, and Chakravarty⁵ (THC) introduced a particular scaling form for $S(k, \omega)$, including parameters for the damping of spin waves, based on the analysis of CHN and on general considerations of analyticity and scaling behavior. In order to set the unknown parameters in the scaling form, they performed a numerical simulation of a classical system whose low-temperature long-wavelength behavior is believed to emulate exactly the QHAF.¹ The scaling form was found to work well in the limited temperature range of the simulations.

It is natural to try to give a more rigorous derivation of

the damping, and since the main damping is believed to come from magnon-magnon scattering, it should be possible to calculate Γ_k in perturbation theory. It is the purpose of this paper to calculate exactly to lowest order the inverse lifetime of the magnons—i.e., the width of the spin-wave peaks in $S(k, \omega)$ —for the 2D Heisenberg antiferromagnet both in the classical and in the quantum case. We will do this in the limit of low temperatures, long wavelengths ($T \rightarrow 0$, $k \rightarrow 0$), and when the spin is large ($S \gg 1$). We believe that our results are also applicable for small S however, including $S = \frac{1}{2}$, as long as the correct quantum-fluctuation-renormalized values are used for the zero-temperature spin-stiffness constant and magnon frequencies.

The results are obtained for various regimes, which are distinguished by the relative sizes of ka and τ ; respectively, the dimensionless wave vector and the dimensionless temperature. In the longest-wavelength regime, we make contact with the scaling forms. All the calculations are done in the case of the 2D Heisenberg antiferromagnet, but the results should be applicable to rotor models as well as to nonlinear sigma models (the correspondence between the various models is given by CHN). These results are also applicable, in principle, to La_2CuO_4 , but they are beyond current capabilities to measure.^{3,4} Finally these results are applicable to molecular-dynamics simulations of the classical lattice rotor model (CLRM).

The analytic methods employed in this paper are similar to the methods used by Harris, Kumar, Halperin, and Hohenberg (HKHH) (Ref. 6) in three dimensions, and, as in three dimensions, their domain of validity is restricted to the regions where the damping is dominated by two-magnon scattering. In 3D, at low temperatures, it was sufficient that ka be small. In two dimensions, however, we must take into account an additional restriction: As a consequence of the Hohenberg-Mermin-Wagner theorem,⁷ there is no long-range order at any finite temperature. As long as there is long-range order at $T = 0$,

however, the spin-wave expansions can still be done locally within regions much smaller than the correlation length ξ . Thus, our calculations are confined to the region where the wave vector is much larger than the inverse correlation length ($k \gg \xi^{-1}$). With this extra restriction the lack of long-range order (LRO) should not be critical. Moreover, since $\xi^{-1} \rightarrow 0$ very rapidly for $\tau \rightarrow 0$ [$\ln(\xi/a) \propto \text{const}/\tau$], there remains a large range of wave vectors where the calculations are valid.

The assumption of long-range order in the ground state at $T=0$ is known rigorously to be correct for the quantum Heisenberg antiferromagnet on a square lattice with nearest-neighbor interactions, for all spins $S \geq 1$.⁸ There is also strong evidence that this is correct for $S = \frac{1}{2}$.⁹

If one includes in the Hamiltonian frustrating interactions, with second-nearest neighbors and further spins, it may be possible for quantum fluctuations to destroy the long-range antiferromagnetic order at $T=0$, in which case our theory would no longer be applicable. Also, if one chooses parameters such that LRO exists at $T=0$, but the quantum fluctuations have almost destroyed the LRO, then there may be a length scale ξ_{quant} large compared to the lattice constant a , such that it is necessary to have $k < \xi_{\text{quant}}^{-1}$ for spin-wave theory to apply. There will also be large renormalizations of the parameters of the spin-wave Hamiltonian due to the quantum fluctuations. For the nearest-neighbor model, however, even for $S = \frac{1}{2}$, it appears that ξ_{quant} is not very different from a .

In order to test our results, we compare them with simulations of the CLRM. THC have performed simulations of the CLRM in a range of temperatures where the correlation length ξ is much smaller than the system size L , and as a practical consequence they could not study the region with $\ln(k\xi) \gg 1$. The analytic expressions developed in this paper, however, are more directly applicable to a lower temperature regime, at wave vectors such that $\ln(k\xi)$ is large. Therefore, we have carried out additional simulations in this lower temperature regime. Although the value of ξ is actually much larger than L , in this regime, it is reasonable to hope that the spin-wave damping for nonzero values of k , in the finite system, are similar to the damping in an infinite system at the same temperature and wave vector. This is because the damping Γ_k in our spin-wave analysis comes primarily from intermediate wave vectors which are $\geq k$.

In our analytic calculation, we follow HKHH and use the Dyson-Maleev¹⁰ (DM) formalism instead of the more familiar Holstein-Primakoff¹¹ (HP) formalism. DM and HP give identical results for the on-shell calculation of the decay rate in the limit $S \rightarrow \infty$, $T \rightarrow 0$. However, DM is much simpler for the off-shell calculations, and, in three dimensions, the self-consistency check works with DM but not with HP. We perform the off-shell calculation mainly to ensure that the DM formalism is stable for off-shell excitations. The off-shell calculation can, in principle, provide the information necessary to determine the shape of the dynamic-correlation function away from the spin-wave peak. However, we do not discuss this here.

Let us now summarize the results in terms of the physical parameters characterizing the model: ρ_S is the zero-

temperature spin-stiffness constant, c is the zero-temperature spin-wave velocity, a is the lattice constant, S is the length of the spin, T is the temperature in units of energy, u_A and u_B are constants of order unity, and $f(\hat{\mathbf{k}})$ is a weak function of the direction of the wave vector \mathbf{k} [$f(\hat{\mathbf{k}}) \approx \frac{1}{5}$].

For the *quantum system* we find the following.

Regime *A* [$k_{\text{min}}(\tau) \ll k \ll (T/\rho_S)^2(T/8\pi\hbar c) \ll a^{-1}$]:

$$\Gamma_k = \frac{\pi ck}{2} \left[\frac{T}{2\pi\rho_S} \right]^2 \left[2 \ln \left[\frac{2\pi\rho_S}{T} \right] + \ln \left[\frac{2}{\pi} \right] + u_A \right], \quad (1.1)$$

regime *B* [$(T/\rho_S)^2(T/8\pi\hbar c) \ll k \ll T/\hbar c \ll a^{-1}$]:

$$\Gamma_k = \frac{\pi ck}{2} \left[\frac{T}{2\pi\rho_S} \right]^2 \left[\ln \left[\frac{T}{\hbar ck} \right] + u_B \right], \quad (1.2)$$

regime *C* [$T/\hbar c \ll k \ll a^{-1}(TS/2\rho_S)^{1/3} \ll a^{-1}$]:

$$\Gamma_k = \frac{0.662\pi}{2} \left[\frac{Tck}{\hbar} \right]^{1/2} \left[\frac{T}{2\pi\rho_S} \right]^2, \quad (1.3)$$

regime *D* [$a^{-1}(TS/2\rho_S)^{1/3} \ll k \ll a^{-1}$]:

$$\Gamma_k = \frac{1.80\pi}{2} \left[\frac{T}{2\pi\rho_S} \right]^2 \frac{T}{\hbar ka \sqrt{f(\hat{\mathbf{k}})}}. \quad (1.4)$$

The existence of a lower bound $k_{\text{min}}(T)$ for the applicability of regime *A* is a consequence of the fact that, at any finite temperature the long-range order is destroyed by thermal fluctuations, and hence the calculations, which rely on a perturbation of an ordered ground state, cannot be valid for infinitely small k at fixed temperature T . The value of k_{min} will be discussed later.

The results given above are derived below explicitly in the limit $T/JS \rightarrow 0$ and $S \rightarrow \infty$. However, we believe that one can relax the condition $S \rightarrow \infty$ provided that one takes into account the renormalization of ρ_S and c due to *quantum* fluctuations. We argue that the scattering of long-wavelength magnons is a purely geometrical process and that the short-wavelength quantum fluctuations can be taken into account by renormalizing the parameters of an effective long-wavelength Hamiltonian; the fact that the damping in regimes *A*, *B*, and *C* only depends on parameters defined at long wavelengths is a consistency check of the argument. In this spirit, we expect that the formulas for the damping should be valid even at small values of the spin S (in particular for $S = \frac{1}{2}$), provided that the correct zero-temperature values of the spin stiffness ρ_S and the spin-wave velocity c are used¹² (since these are the physical parameters describing the effective long-wavelength Hamiltonian). This prescription is valid for regimes *A*, *B*, and *C* because, in these regimes, the damping can be expressed solely in terms of the long-wavelength parameters. By contrast, in regime *D*, one cannot express the damping without reference to the short-wavelength parameters of the system, either through a or through S . Also, the damping depends on the curvature of the spectrum—via the dimensionless function $f(\hat{\mathbf{k}})$ —only in regime *D*. Presumably, the quan-

tum fluctuations will also renormalize the curvature in a way not related to the renormalization of the slope c . We have not attempted to compute the effects of quantum renormalization in regime D .

For the *classical system* we find the following results:

Regime A_{cl} [$k_{\min}(T)a \ll ka \ll e^{\pi/2}(T/\rho_S)^2/\sqrt{2\pi}$]:

$$\Gamma_k = \frac{\pi ck}{2} \left[\frac{T}{2\pi\rho_S} \right]^2 [2 \ln(2\pi\rho_S/T) + \ln(2/\pi) + u_A], \quad (1.5)$$

Regime B_{cl} [$e^{\pi/2}(T/\rho_S)^2/\sqrt{2\pi} \ll ka \ll 1$]:

$$\Gamma_k = \frac{\pi ck}{2} \left[\frac{T}{2\pi\rho_S} \right]^2 [\ln(1/ka) + \ln(\sqrt{32}e^{\pi/2}) + u_{B_{cl}}]. \quad (1.6)$$

Similar results are expected for the classical rotor model, except that the constant $u_{B_{cl}}$ in Eq. (1.6) will be different than for the antiferromagnet.

We note that the equations of motion for the classical antiferromagnet are identical to those of the quantum antiferromagnet, if one takes the limit $S \rightarrow \infty$ in the QHAF, and suitably rescales the coupling constant J and the temperature T . Our formulas for the damping may differ, in principle, in the two cases because the classical formulas are supposed to be valid in the limit where first $S \rightarrow \infty$, and then $(T/\rho_S) \rightarrow 0$, whereas the formulas for the QHAF are derived in the limit where $(T/\rho_S) \rightarrow 0$ faster than S^{-1} .

We see that, in fact, there is a difference in the argument of the logarithm in the formulas (1.2) and (1.6) for the damping in the intermediate-wavelength regimes B and B_{cl} . By contrast, formulas (1.1) and (1.5) for the damping in the long-wavelength regimes A and A_{cl} are identical, regardless of the value of S in the QHAF.

Thus far, we have omitted from our formulas the effects of renormalization of the spin-stiffness constant and magnon velocity due to thermal fluctuations. At low temperatures, these effects become important only at very long wavelengths, specifically for $k < k_{\min}$, where $k_{\min} \rightarrow 0$ faster than any power of T , for $T \rightarrow 0$. Thus, for $T \rightarrow 0$, this renormalization becomes important only at the long-wavelength end of regime A or A_{cl} . We argue below that the correct way to include the renormalization at long wavelengths is to replace the quantity ck in Eqs. (1.1) or (1.5) by the actual, temperature-renormalized spin-wave frequency $\omega_k(T)$, and to replace ρ_S by the renormalized stiffness constant $\rho_S(k, T)$ at wave vector k and temperature T . According to the renormalization-group analysis, the value of $\rho_S(k, T)$ may be written in the asymptotic form $\rho_S(k, T) \sim (T/2\pi)\ln(k\xi)$ for $k\xi \gg 1$, provided that k is small compared to the *upper* limits quoted above for regime B or B_{cl} . A somewhat better formula for $\rho_S(k, T)$, proposed in CHN, which appears to work for values of $k\xi$ down to $k\xi \approx 1$, is

$$\rho_S(k, T) = \frac{T}{2\pi} \left\{ \delta + \frac{1}{2} \ln[1 + (k\xi)^2] \right\}, \quad (1.7)$$

where δ is a constant. In a previous paper⁵ (THC), we

found that the spin-wave frequency was given most accurately when δ is chosen to be $\delta \approx 1.7$. If Eq. (1.7) is now used for ρ_S in our formulas for the spin-wave damping, we find in regime A or A_{cl} , the scaling formula

$$\Gamma_k/\omega_k = \frac{\pi}{2} \frac{\{2 \ln[\delta + \frac{1}{2} \ln(1+q^2)] + \ln(2/\pi) + u_A\}}{[\delta + \frac{1}{2} \ln(1+q^2)]^2}, \quad (1.8)$$

where $q \equiv k\xi$. This formula should be valid at low temperatures for $k\xi \gtrsim 1$ and k less than the upper bounds quoted above for regime A or A_{cl} .

Although renormalization of the spin stiffness should be negligible in regime B or B_{cl} at low temperatures, Eq. (1.7) does give significant renormalization of $\rho_S(k, T)$ in this wavelength regime at the higher temperatures used in our computer simulations of the CLRM. Even though from a theoretical point of view we cannot rule out the importance of other corrections at these higher temperatures, we do find that there is a significant improvement in the agreement between theory and simulation if we use Eq. (1.7) in the formula for Γ_k/ω_k in regime B_{cl} .

The remainder of this paper will be organized as follows. In Sec. II, we shall first present the salient aspects of the formalism (the reader is referred to HKHH for a more extensive discussion of it). Then, in Sec. III, we perform the quantum calculation without imposing self-consistency. We do the calculation in four regimes B_1 , B_2 , C , and D with different approximations in each. The results of B_1 and B_2 are identical and we call the merged regime B' . In Sec. IV we impose self-consistency and check for the off-shell stability of the calculation. The self-consistency condition splits regime B' in two regimes A and B , and we end up with four different regimes as presented above. In Sec. V we take the classical limit by letting the spin S go to infinity; then we refine the classical expressions somewhat, by using the detailed mapping of CHN between the static properties of the quantum and classical systems. We thus obtain the results for the decay rate in the two classical regimes: A_{cl} and B_{cl} . We also make some further observations on the expected effects of renormalization due to thermal fluctuations. Finally, in Sec. VI we compare the results of our calculations with a simulation of the CLRM. The summary, given in Sec. VII, includes comparison with the work of other authors.

II. FORMALISM

The model that we study is defined by

$$H = J \sum_{\langle i,j \rangle} \mathbf{S}_i \cdot \mathbf{S}_j, \quad (2.1)$$

where the definition of J differs from that of Ref. 6 by a factor of 2. The sum $\langle i,j \rangle$ runs over bonds in a square lattice whose lattice spacing is a . Sites “ i ” belong to the sublattice “ a ” (“up”) and sites “ j ” belong to the sublattice “ b ” (“down”). Sublattices a and b are both square lattices tilted at an angle of 45° from the original lattice, their lattice spacing is $d = \sqrt{2}a$, and each sublattice consists of N sites. The units are such that the positive quantity J has dimensions of energy and that the spin opera-

tors \mathbf{S}_i and \mathbf{S}_j are dimensionless.

The Dyson-Maleev transformation expresses the spin Hamiltonian (2.1) in terms of boson operators. In the case of nonfrustrated antiferromagnetic coupling, the correspondence is

$$S_i^z = S - a_i^\dagger a_i, \quad (2.2a)$$

$$S_i^+ = (2S)^{1/2} a_i - (2S)^{-1/2} a_i^\dagger a_i a_i, \quad (2.2b)$$

$$S_i^- = (2S)^{1/2} a_i^\dagger, \quad (2.2c)$$

$$S_j^z = -S + b_j^\dagger b_j, \quad (2.2d)$$

$$S_j^+ = (2S)^{1/2} b_j^\dagger - (2S)^{-1/2} b_j^\dagger b_j^\dagger b_j, \quad (2.2e)$$

$$S_j^- = (2S)^{1/2} b_j, \quad (2.2f)$$

where a_i and b_i are boson annihilation operators. The Hamiltonian (2.1) is written in terms of the boson operators by substituting the spin operators as in Eq. (2.2). The resulting non-Hermitian Hamiltonian has a zeroth-order term E'_0 , a second-order term H'_0 , a fourth-order term V' , and no higher-order term. It was established by Dyson¹³ that the expectation value of spin operators was equal to the expectation value of the corresponding boson operators if one was careful not to count the “unphysical” boson states. The unphysical boson states are those where there exists a site in the lattice populated by more than $2S$ bosons. Within this constraint, the correspondence is exact. However, in order to do the calculations, HKHH were compelled to make the two following approximations. The first one was to treat the quartic terms in a perturbation expansion. The second one was to ignore the requirement to project out the unphysical states. We refer the reader to HKHH for a full discussion of the consequences of these approximations.

In order to simplify the Hamiltonian, one introduces the Fourier transforms of the boson operators,

$$a_{\mathbf{k}} = N^{-1/2} \sum_i e^{-i\mathbf{k}\cdot\mathbf{r}_i} a_i, \quad (2.3a)$$

$$b_{\mathbf{k}} = N^{-1/2} \sum_j e^{-i\mathbf{k}\cdot\mathbf{r}_j} b_j, \quad (2.3b)$$

where each summation is restricted to the relevant sublattice. The quadratic part of the Hamiltonian is then given by

$$H'_0 = \hbar\omega_E \sum_{\mathbf{p}} (a_{\mathbf{p}}^\dagger a_{\mathbf{p}} + b_{\mathbf{p}}^\dagger b_{\mathbf{p}} + \gamma_{\mathbf{p}} a_{\mathbf{p}}^\dagger b_{-\mathbf{p}}^\dagger + \gamma_{\mathbf{p}} a_{\mathbf{p}} b_{-\mathbf{p}}), \quad (2.4)$$

where

$$\hbar\omega_E \equiv JzS, \quad (2.5)$$

and z is the number of nearest neighbors, and for the square lattice we have

$$\gamma_{\mathbf{p}} = \cos(p_x d/2) \cos(p_y d/2). \quad (2.6)$$

In the remainder of this section and the following two, unless otherwise noted, the wave vectors will be dimensionless quantities. The quantity k will always be understood to represent the product kd .

Then one goes on to diagonalize the quadratic part of

the Hamiltonian H'_0 with the transformation

$$a_{\mathbf{p}} = l_{\mathbf{p}} \alpha_{\mathbf{p}}^\dagger + m_{\mathbf{p}} \beta_{-\mathbf{p}}, \quad (2.7a)$$

$$b_{\mathbf{p}} = m_{\mathbf{p}} \alpha_{\mathbf{p}}^\dagger + l_{\mathbf{p}} \beta_{-\mathbf{p}}, \quad (2.7b)$$

where

$$l_{\mathbf{p}} = [(1 + \epsilon_{\mathbf{p}})/2\epsilon_{\mathbf{p}}]^{1/2}, \quad (2.8a)$$

$$m_{\mathbf{p}} = -[(1 - \epsilon_{\mathbf{p}})/2\epsilon_{\mathbf{p}}]^{1/2}, \quad (2.8b)$$

with

$$\epsilon_{\mathbf{p}} = (1 - \gamma_{\mathbf{p}}^2)^{1/2} \quad (2.9)$$

denoting a dimensionless energy. The quadratic Hamiltonian is then simply given by

$$H_0 = \hbar\omega_E \sum_{\mathbf{p}} \epsilon_{\mathbf{p}} (\alpha_{\mathbf{p}}^\dagger \alpha_{\mathbf{p}} + \beta_{\mathbf{p}}^\dagger \beta_{\mathbf{p}}). \quad (2.10)$$

The quartic Hamiltonian is very complicated and has nine interaction vertices; it is given in full detail by Eq. (2.17b) of HKHH.

HKHH then introduce thermodynamic Green's functions for the α and β magnons similar to the Nambu matrices for superconductors,

$$G_{\alpha\alpha}(\mathbf{k}, t) = -i \langle T(\alpha_{\mathbf{k}}(t) \alpha_{\mathbf{k}}^\dagger(0)) \rangle, \quad (2.11a)$$

$$G_{\alpha\beta}(\mathbf{k}, t) = -i \langle T(\alpha_{\mathbf{k}}(t) \beta_{-\mathbf{k}}(0)) \rangle, \quad (2.11b)$$

$$G_{\beta\alpha}(\mathbf{k}, t) = -i \langle T(\beta_{-\mathbf{k}}^\dagger(t) \alpha_{\mathbf{k}}^\dagger(0)) \rangle, \quad (2.11c)$$

$$G_{\beta\beta}(\mathbf{k}, t) = -i \langle T(\beta_{-\mathbf{k}}^\dagger(t) \beta_{-\mathbf{k}}(0)) \rangle, \quad (2.11d)$$

where the angular brackets denote an average over an ensemble at a temperature $(\beta)^{-1}$, and here T is the time-ordering operator. The frequency-dependent functions are defined by Fourier transforms

$$G_{\mu\nu}(\mathbf{k}, z) = \hbar^{-1} \int_0^{-i\beta\hbar} G_{\mu\nu}(\mathbf{k}, t) e^{izt} dt, \quad (2.12)$$

for $z = 2\pi ni(\beta\hbar)^{-1}$, with n an integer. For other values of z , $G_{\mu\nu}(\mathbf{k}, z)$ is defined by the usual analytic continuation procedure.

HKHH go on to define the self-energy $\Sigma_{\mu\nu}(\mathbf{k}, z)$ through the Dyson equation, in the usual way, and show that it is small compared to the unperturbed energy so that to leading order the Green's function can be written as

$$G_{\alpha\alpha}(\mathbf{k}, z) = [\hbar z - \hbar\omega_E \epsilon_{\mathbf{k}} - \Sigma_{\alpha\alpha}(\mathbf{k}, z)]^{-1}, \quad (2.13a)$$

$$G_{\beta\beta}(\mathbf{k}, z) = [-\hbar z - \hbar\omega_E \epsilon_{\mathbf{k}} - \Sigma_{\beta\beta}(\mathbf{k}, z)]^{-1}, \quad (2.13b)$$

$$G_{\alpha\beta}(\mathbf{k}, z) = -\Sigma_{\alpha\beta}(\mathbf{k}, z) [\hbar z - \hbar\omega_E \epsilon_{\mathbf{k}} - \Sigma_{\alpha\alpha}(\mathbf{k}, z)]^{-1} \\ \times [\hbar z + \hbar\omega_E \epsilon_{\mathbf{k}} + \Sigma_{\beta\beta}(\mathbf{k}, z)]^{-1}, \quad (2.13c)$$

$$G_{\beta\alpha}(\mathbf{k}, z) = -\Sigma_{\beta\alpha}(\mathbf{k}, z) [\hbar z - \hbar\omega_E \epsilon_{\mathbf{k}} - \Sigma_{\alpha\alpha}(\mathbf{k}, z)]^{-1} \\ \times [\hbar z + \hbar\omega_E \epsilon_{\mathbf{k}} + \Sigma_{\beta\beta}(\mathbf{k}, z)]^{-1}. \quad (2.13d)$$

Thus the damping of the α magnon is determined by

$$\Sigma''_{\alpha\alpha}(\mathbf{k}, \omega) \equiv \text{Im} \Sigma_{\alpha\alpha}(\mathbf{k}, \omega - i0^+) \equiv \hbar \Gamma(\mathbf{k}, \omega). \quad (2.14)$$

If $\omega_{\mathbf{k}}$ is the center frequency of the magnon with wave

vector \mathbf{k} , then the quantity $\Gamma_{\mathbf{k}}$, defined by

$$\Gamma_{\mathbf{k}} \equiv \Gamma(\mathbf{k}, \omega)|_{\omega=\omega_{\mathbf{k}}}, \quad (2.15)$$

enters the expression for the correlation function of the staggered magnetization as the half width at half maximum of the Lorentzian shape. Of course, $\omega_{\mathbf{k}}$, to lowest order in the perturbation, is equal to $\omega_E \varepsilon_{\mathbf{k}}$. We shall refer to $\Gamma_{\mathbf{k}}$ as the on-shell magnon damping. (Note that $\Gamma_{\mathbf{k}}$ is actually one-half the decay rate for magnon occupation number or intensity.) The form of $\Gamma(\mathbf{k}, \omega)$ for $\omega \neq \omega_E \varepsilon_{\mathbf{k}}$, which we shall sometimes refer to as the off-

shell magnon damping, can also be of some interest because it enters, indirectly, into a calculation of the form of the tails of the staggered-spin correlation function $S(\mathbf{k}, \omega)$, far from the spin-wave peaks. Calculations of the off-shell magnon damping will be used in the present paper, however, only as an intermediate step in the calculations when we wish to include self-consistently the effects of magnon damping in our scattering states.

In order to calculate $\Sigma''_{\alpha\alpha}(\mathbf{k}, \omega)$, HKHH set up a perturbation expansion. The expansion parameters are the temperature T , the inverse of the number of nearest neighbors $1/z$, and the inverse of the length of the spin $1/S$. To lowest nonvanishing order, the decay rate is given by

$$\Gamma(\mathbf{k}, \omega) = \frac{\pi\omega_E}{(4NS)^2} (1 - e^{-2\tilde{\omega}/\tau}) \sum_{\mathbf{p}, \mathbf{s}} n_{\mathbf{p}} (1 + n_{\mathbf{r}}) (1 + n_{\mathbf{s}}) \times [\delta(\tilde{\omega} + \varepsilon_{\mathbf{p}} - \varepsilon_{\mathbf{r}} - \varepsilon_{\mathbf{s}}) M_{22}(\mathbf{k}, \mathbf{p}, \mathbf{r}, \mathbf{s}) + e^{2\tilde{\omega}/\tau} \delta(-\tilde{\omega} + \varepsilon_{\mathbf{p}} - \varepsilon_{\mathbf{r}} - \varepsilon_{\mathbf{s}}) M_{31}(\mathbf{k}, \mathbf{p}, \mathbf{r}, \mathbf{s})], \quad (2.16)$$

where $\tilde{\omega}$ is the dimensionless frequency of the incoming magnon,

$$\tilde{\omega} = \omega / \omega_E,$$

and τ is the dimensionless temperature,

$$\tau = 2T / JzS,$$

and momentum conservation is understood, so that $\mathbf{k} + \mathbf{p} = \mathbf{r} + \mathbf{s}$. The occupation numbers are given by

$$n_{\mathbf{p}} = (e^{2\varepsilon_{\mathbf{p}}/\tau} - 1)^{-1}. \quad (2.17)$$

The squared matrix elements M_{22} and M_{31} correspond, respectively, to processes with two magnons in and two magnons out (M_{22}), and processes with three magnons in and one out—or the converse—(M_{31}). They are given, in the long-wavelength limit, by

$$M_{22} = 2[(1 - \hat{\mathbf{k}} \cdot \hat{\mathbf{p}})(1 - \hat{\mathbf{r}} \cdot \hat{\mathbf{s}}) + (1 - \hat{\mathbf{k}} \cdot \hat{\mathbf{r}})(1 - \hat{\mathbf{p}} \cdot \hat{\mathbf{s}}) + (1 - \hat{\mathbf{k}} \cdot \hat{\mathbf{s}})(1 - \hat{\mathbf{p}} \cdot \hat{\mathbf{r}})], \quad (2.18)$$

$$M_{31} = -2[(1 + \hat{\mathbf{k}} \cdot \hat{\mathbf{p}})(1 - \hat{\mathbf{r}} \cdot \hat{\mathbf{s}}) + (1 + \hat{\mathbf{k}} \cdot \hat{\mathbf{r}})(1 - \hat{\mathbf{p}} \cdot \hat{\mathbf{s}}) + (1 + \hat{\mathbf{k}} \cdot \hat{\mathbf{s}})(1 - \hat{\mathbf{p}} \cdot \hat{\mathbf{r}})]. \quad (2.19)$$

Before starting the calculation, let us set up some notation that will be useful throughout the next section.

The spectrum is linear at small wave vectors and we can write

$$\varepsilon_{\mathbf{k}} \approx \frac{k}{2} [1 - k^2 g(\hat{\mathbf{k}}) / 32], \quad (2.20)$$

where the dependence on angle is given by

$$g(\hat{\mathbf{k}}) = 1 + 2k_x^2 k_y^2 / k^4 + (k_x^4 + k_y^4) / 3k^4, \quad (2.21)$$

and g has a weak angle dependence, $\frac{4}{3} \leq g \leq \frac{5}{3}$. We also need to define the gradient of $\varepsilon_{\mathbf{k}}$ to perform expansions,

$$\mathbf{v}_{\mathbf{k}} \equiv 2\nabla_{\mathbf{k}} \varepsilon_{\mathbf{k}}. \quad (2.22)$$

With this definition, $v_{\mathbf{k}}$ tends to unity as k tends to zero,

$$v_{\mathbf{k}} \approx 1 - k^2 f(\hat{\mathbf{k}}), \quad (2.23)$$

and $f(\hat{\mathbf{k}})$ is given by

$$f(\hat{\mathbf{k}}) = [3 + 6k_x^2 k_y^2 / k^4 + 4(k_x^4 + k_y^4) / k^4 - (k_x^6 + k_y^6) / 3k^6] / 32. \quad (2.24)$$

The angle dependence of f is very weak; $f \approx \frac{1}{3}$ for all angles.

III. LOW-TEMPERATURE LONG-WAVELENGTH APPROXIMATION IN THE QUANTUM REGIME

In this section we will calculate the first Born approximation for the decay rate of an on-shell magnon neglecting the finite lifetime of intermediate magnons. By “on-shell” we mean that $\tilde{\omega} = \varepsilon_{\mathbf{k}}$. The scattering process that we will study is

$$\mathbf{p} + \mathbf{k} \rightarrow \mathbf{s} + \mathbf{r} \quad (3.1)$$

and the momentum transfer \mathbf{q} is defined by

$$\mathbf{s} = \mathbf{k} + \mathbf{q} \quad (3.2)$$

and

$$\mathbf{r} = \mathbf{p} - \mathbf{q}. \quad (3.3)$$

The scattering surface is a surface in the momentum transfer plane defined by the conservation of energy,

$$\varepsilon_{\mathbf{k}} + \varepsilon_{\mathbf{p}} - \varepsilon_{\mathbf{k}+\mathbf{q}} - \varepsilon_{\mathbf{p}-\mathbf{q}} = 0. \quad (3.4)$$

There is a center of inversion symmetry at $\mathbf{I} = (\mathbf{p} - \mathbf{k}) / 2$ such that if \mathbf{q} belongs to the surface, then $\mathbf{q}' = 2\mathbf{I} - \mathbf{q}$ also belongs to the surface. We will refer the reader to HKHH for an extensive discussion of the scattering surface; we will only present their main conclusions.

Depending on the relative size of p and q , there exist

different types of scattering surfaces. For instance, when the two momenta are of "comparable size" (more specifically, when $k^3 < p < k^{1/3}$), then one can expand to first order each term in Eq. (3.4) and the scattering surface can be described as an ellipse:

$$|\mathbf{k} + \mathbf{q}| + |\mathbf{p} - \mathbf{q}| = p + k . \quad (3.5)$$

This description is valid for all the momenta p in this interval except for an infinitesimal range such that $\hat{\mathbf{p}} \cdot \hat{\mathbf{k}} \sim 1$. For our purpose the description by an ellipse Eq. (3.5) is accurate enough.

By contrast, when either of the two momenta is much

greater than the other one ($p < k^3$ or $k^{1/3} < p$), then the scattering surface consists of two disjoint parts. In the case where $p < k^3$, the two disjoint parts correspond to either $\mathbf{q} \sim -\mathbf{k}$ or $q \sim 0$. For the part where $\mathbf{q} \sim -\mathbf{k}$, one can do a Taylor expansion of $\varepsilon_k - \varepsilon_r$ and use only the linear term for ε_p and ε_s ; one gets

$$\delta(\varepsilon_k + \varepsilon_p - \varepsilon_r - \varepsilon_s) = 2\delta(p - s - v_k(p\mu - s\nu)) , \quad (3.6)$$

where $\mu \equiv \hat{\mathbf{v}}_k \cdot \hat{\mathbf{p}}$ and $\nu \equiv \hat{\mathbf{v}}_k \cdot \hat{\mathbf{s}}$.

In the low-temperature long-wavelength regime, the quantity that we have to evaluate is, in the lowest Born approximation,

$$\Gamma_{\mathbf{k}} \equiv \Gamma(\bar{\omega} = \varepsilon_{\mathbf{k}}, \mathbf{k}) , \quad (3.7)$$

$$\Gamma_{\mathbf{k}} = \frac{\pi\omega_E}{16S^2(2\pi)^4} (1 - e^{-2\varepsilon_{\mathbf{k}}/\tau}) \int d^2q d^2p n_p(1+n_r)(1+n_s) M_{22}(\mathbf{k}, \mathbf{p}, \mathbf{r}, \mathbf{s}) \delta(\Delta\varepsilon) , \quad (3.8)$$

where $\Delta\varepsilon = \varepsilon_{\mathbf{k}} + \varepsilon_p - \varepsilon_r - \varepsilon_s$.

For on-shell scattering, the matrix element M_{31} does not give any contribution because it cannot conserve energy and momentum at the same time (this is due to the fact that a convex spectrum does not allow spontaneous decay of one magnon into three; see HKHH Appendix E for more details).

We now proceed to evaluate the lowest Born approximation for the on-shell magnon decay rate $\Gamma_{\mathbf{k}}$. For each value of k and τ there will be a range of values for p that will give the major contribution to $\Gamma_{\mathbf{k}}$. Depending on how these values compare with k , most of the scattering will come from surfaces with very different shapes. As a first guess, one may think that the major contribution always comes from thermal magnons, $p \simeq \tau$. This is actually the case in three dimensions (Ref. 6) and in some of the regimes in two dimensions. As a direct consequence of the preeminence of thermal momenta in three dimensions, HKHH were led to define four regimes, it will be convenient for the calculations to follow their definition as follows (their regime *A* and *B* correspond to our regimes B_1 and B_2 , respectively).

$$\varepsilon_k \ll \tau^3 \ll 1 , \quad (3.9)$$

we will see that the dominant contribution to the decay rate comes from values of the incoming magnon p such that $k < p < \tau$. For these values of p , the scattering surface consists alternatively of a single ellipse and of two disjoint pieces.

In regime B_2 , defined by

$$\tau^3 \ll \varepsilon_k \ll \tau \ll 1 , \quad (3.10)$$

we find that, as in regime B_1 , the dominant momenta for p occur in the range $k < p < \tau$. For all these values the scattering surface is an ellipse and the temperature is still large enough ($\tau \gg \varepsilon_k$) so that the reverse processes cannot be neglected, i.e., $\exp(-2\varepsilon_k/\tau)$ is of order unity.

In regime *C*, defined by

$$\tau \ll \varepsilon_k \ll \tau^{1/3} \ll 1 , \quad (3.11)$$

the important momenta for p are not anymore in a whole range as in B_1 or B_2 but rather only around the thermal momentum $p \simeq \tau$. The scattering surface is as in B_2 an ellipse, but the reverse processes can now be neglected.

In regime *D*, defined by

$$\tau^{1/3} \ll \varepsilon_k \ll 1 , \quad (3.12)$$

as in regime *C*, only the thermal momenta contribute to the leading term in $\Gamma_{\mathbf{k}}$. The relevant scattering surface is disjoint, and we will see that this is the only regime in which the scattering rate depends on the orientation of k in the Brillouin zone.

In three dimensions HKHH find four different forms for the decay rate corresponding to the four regimes. In two dimensions, however, regimes B_1 and B_2 will yield the same form for the decay rate. We will consolidate them into regime B' ,

$$\text{regime } B': \varepsilon_k \ll \tau \ll 1 . \quad (3.13)$$

The lack of difference between regime B_1 and regime B_2 in two dimensions originates in the fact that the momenta p which give the leading-order contribution to $\Gamma_{\mathbf{k}}$ are spread out in a whole range which spans the different types of scattering surfaces, whereas in three dimensions only the thermal momenta are important. Another difference between two dimensions and three dimensions is that the first Born approximation is self-consistent in each of the four regimes in three dimensions, whereas in two dimensions the self-consistency condition will come in to split regime B' in two parts, and will leave the other regimes unchanged. The self-consistent calculation will be done in Sec. IV.

We will now present the calculation of $\Gamma_{\mathbf{k}}$ in each of the regimes. Even though regime B_1 and regime B_2 will turn out to be equivalent in the first Born approximation, we still keep the distinction because we use a slightly different approximation to compute the decay in each one.

A. Regime B_1 , $\varepsilon_k \ll \tau^3 \ll 1$

One can expand the exponential involving ε_k in Eq. (3.8) and write

$$\Gamma_k = \frac{\pi \omega_E \varepsilon_k}{8S^2(2\pi)^4 \tau} \int d^2 q d^2 p n_p (1+n_r)(1+n_s) \times M_{22}(k, p, r, s) \delta(\Delta\varepsilon). \quad (3.14)$$

We can divide the p integral in different regions within which the scattering surface can be easily approximated. The three regions are

$$\begin{aligned} \text{region 1: } & 0 < p < \lambda_2 k^3, \\ \text{region 2: } & \lambda_2 k^3 < p < \lambda_1 k^{1/3}, \\ \text{region 3: } & \lambda_1 k^{1/3} < p < 2\sqrt{\pi}, \end{aligned} \quad (3.15)$$

where λ_1 and λ_2 are numerical constants which we are free to adjust so that this arbitrary partitioning be optimally chosen. Final results must be independent of any reasonable (finite and fixed) choice of λ_1 and λ_2 . The value $2\sqrt{\pi}$ in region 3 is chosen so as to conserve the area of the Fermi surface when one replaces the original square by a disk (this approximation should be valid in the limit of long wavelengths).

In *region 1* ($0 < p < \lambda_2 k^3$), the scattering surface consists of two disjoint parts, one where $q \simeq 0$, and one where $q \simeq -\mathbf{k}$. These two parts are the symmetric of one another with respect to the center of symmetry $\mathbf{I} = (\mathbf{p} - \mathbf{k})/2$. This symmetry transforms \mathbf{r} into \mathbf{s} and *vice versa*. Since the integrand of Eq. (3.14) is unchanged under this transformation, the integration over the part of the surface $q \simeq 0$ is equal to the integration over the other part. We can then take twice the contribution of the surface $q \simeq -\mathbf{k}$. For this surface, we have $s \simeq 0$ and $r \simeq k$, so that we can expand the argument of the energy-conserving δ function as in Eq. (3.6):

$$\delta(\varepsilon_k + \varepsilon_p - \varepsilon_r - \varepsilon_s) = 2\delta(p - s - v_k(p\mu - s\nu)), \quad (3.16)$$

where $\mu \equiv \hat{\mathbf{v}}_k \cdot \hat{\mathbf{p}}$ and $\nu \equiv \hat{\mathbf{v}}_k \cdot \hat{\mathbf{s}}$. We can also expand all the exponentials because all the momenta are small compared to the thermal momentum τ . Finally, if we use the long-wavelength expression for M_{22} valid for $r \simeq k \gg s, q$, i.e.,

$$M_{22}(k, p, r, s) = 4(1-\mu)(1-\nu), \quad (3.17)$$

the integral for the decay rate becomes

$$\Gamma_k^{(1)} = \frac{\omega_E \tau^2}{2S^2(2\pi)^3} \int d^2 s d^2 p \frac{(1-\nu)(1-\mu)}{ps} \times \delta(p - s - v_k(p\mu - s\nu)). \quad (3.18)$$

One can then use the δ function to perform the angular s integration; one writes

$$\delta(p - s - v_k(p\mu - s\nu)) = \delta(\nu - \nu_0) / s\nu_k,$$

where

$$\nu_0 \equiv \frac{s - p(1 - v_k \mu)}{s\nu_k}.$$

The condition $|\nu_0| \leq 1$ then imposes restrictions on the radial integral, $s^a < s < s^b$, where

$$s^a \equiv \frac{p(1 - \mu v_k)}{1 + v_k}$$

and

$$s^b \equiv \frac{p(1 - \mu v_k)}{1 - v_k}.$$

The radial s integration can be done exactly leaving only a simple integration for p . The result for the contribution of region 1 in regime B_1 is

$$\Gamma_k^{(1)} = \frac{2\omega_E \varepsilon_k^3 \tau^2 \lambda_2}{\pi S^2}. \quad (3.19)$$

This contribution will be negligible compared to the contribution coming from the second region, which we proceed to compute now.

In *region 2* ($\lambda_2 k^3 < p < \lambda_1 k^{1/3}$), all the exponentials can again be expanded, but now the scattering surface is well described by an ellipse. We will introduce elliptical coordinates in order to do the integrations. Let us first make a change of variable ($q \rightarrow q'$) in the momentum-transfer plane—a simple shift of the origin—so that the center of the ellipse lies at the origin in the new coordinates:

$$\mathbf{q}' = \mathbf{q} - \mathbf{I}.$$

Then one chooses the x axis to lie along the major axis of the ellipse. The separation between the foci is given by $2c$ where

$$\mathbf{c} = (\mathbf{p} + \mathbf{k})/2.$$

One then introduces elliptical coordinates in the classical way:

$$q'_x = c \cosh u \cos v, \quad (3.20a)$$

$$q'_y = c \sinh u \sin v, \quad (3.20b)$$

where the new parameters u and v have for range: $0 < u < \infty$ and $0 < v < 2\pi$. The advantage of this representation is that the δ function simply corresponds to a fixed value of u , and that r and s have the following simple expressions:

$$r = c(\cosh u - \cos v) = |\mathbf{c} - \mathbf{q}'|, \quad (3.21a)$$

$$s = c(\cosh u + \cos v) = |\mathbf{c} + \mathbf{q}'|; \quad (3.21b)$$

also, the volume element becomes

$$d^2 q' = c^2 (\cosh^2 u - \cos^2 v) du dv.$$

One can then write

$$\delta(\Delta\varepsilon) = \delta(\cosh u - a/c)/c,$$

and a is the average of the lengths of p and k , $a \equiv (p+k)/2$. We use for M_{22} an expression valid for on-shell scattering in the limit of long wavelengths.⁶

$$M_{22}(k, p, r, s) = 2(\varepsilon_k \varepsilon_p \varepsilon_r \varepsilon_s)^{-1} [\varepsilon_k^2 \varepsilon_p^2 (1 - \hat{\mathbf{k}} \cdot \hat{\mathbf{p}})^2 + \varepsilon_k^2 \varepsilon_r^2 (1 - \hat{\mathbf{k}} \cdot \hat{\mathbf{r}})^2 + \varepsilon_k^2 \varepsilon_s^2 (1 - \hat{\mathbf{k}} \cdot \hat{\mathbf{s}})^2] . \quad (3.22)$$

In this form the u integration is trivially done, and it is possible to do all the v integrations. The result for the first term in M_{22} is particularly simple and gives a contribution to the decay which is

$$\delta\Gamma_k = \frac{\omega_E \varepsilon_k \tau^2}{4\pi S^2} \int_{\lambda_2 k^3}^{\lambda_1 k^{1/3}} \frac{dp}{k+p} . \quad (3.23)$$

It is transparent to see in Eq. (3.23) that the leading contribution comes from momenta in the range $k < p < \lambda_1 k^{1/3}$. The second and third terms in M_{22} are more difficult to evaluate exactly, but their leading contribution can be shown to be just half that of the first term and to come from the same range of momenta. So, to leading order, the total decay rate due to scattering of magnons with momentum p such that $0 < p < \lambda_1 k^{1/3}$ is

$$\Gamma_k^{(2)} = \frac{\omega_E \varepsilon_k \tau^2}{2\pi S^2} \ln \left[\frac{\lambda_1 k^{1/3}}{k} \right] . \quad (3.24)$$

This is independent of the choice of λ_2 .

In *region 3* ($\lambda_1 k^{1/3} < p < 2\sqrt{\pi}$), the contribution can be calculated in a manner similar to region 1. The two disconnected parts of the scattering surface give the same contribution to the scattering rate so that we need to do the integration only for one of them. We choose the one corresponding to $q \sim 0$ which implies ($p \sim r \gg k, s$). In this region the expression for M_{22} in Eq. (3.22) simplifies and gives [we could also use Eq. (3.17) and get the same result]

$$M_{22} = \frac{4\varepsilon_k}{\varepsilon_s} (1 - \hat{\mathbf{k}} \cdot \hat{\mathbf{p}})^2 .$$

The expression for Γ_k is then

$$\Gamma_k^{(3)} = \frac{\omega_E \varepsilon_k^2}{2S^2 (2\pi)^3} \int_{s=0} d^2s d^2p n_p (1+n_p) \frac{(1-\mu)^2}{\varepsilon_s^2} \times \delta(k-s-v_p(k\mu-sv)) , \quad (3.25)$$

where $\mu \equiv \hat{\mathbf{v}}_p \cdot \hat{\mathbf{k}}$ and $\nu \equiv \hat{\mathbf{v}}_p \cdot \hat{\mathbf{s}}$. The s integration can now be performed as in the first case, and the remaining p integral is

$$\Gamma_k^{(3)} = \frac{\omega_E \varepsilon_k}{2\pi S^2} \int_{\lambda_1 k^{1/3}}^{2\sqrt{\pi}} dp p n_p (1+n_p) , \quad (3.26)$$

which can then be evaluated in the limit $k \ll \tau^3$ to give

$$\Gamma_k^{(3)} = \frac{\omega_E \varepsilon_k \tau^2}{2\pi S^2} \ln \left[\frac{\tau}{\lambda_1 k^{1/3}} \right] . \quad (3.27)$$

Hence we have for regime B_1 the sum of the contributions for the three regions:

$$\Gamma_k = \frac{\omega_E \varepsilon_k \tau^2}{2\pi S^2} \ln(\tau/k) . \quad (3.28)$$

This final result is independent of the constants λ_1 and λ_2

and the main contribution has been shown to come from the momenta p such that $k < p < \tau$.

B. Regime B_2 , $\tau^3 \ll \varepsilon_k \ll \tau \ll 1$

As for regime B_1 we look at the contribution from different regions corresponding to different scattering surfaces.

In *region 1*, $p < \lambda_2 k^3$, the scattering surface consists of two disjoint pieces and the calculation goes exactly as in the preceding case. The decay rate contributed by this region is equal to Eq. (3.19), which will again be negligible compared to the leading-order contribution.

In *region 2*, $\lambda_2 k^3 < p < \lambda_1 k^{1/3}$, the scattering surface is approximated by an ellipse. We must compute the decay rate given by Eq. (3.14) where M_{22} is given by Eq. (3.22). In region 2, we cannot expand the exponentials in n_r and n_s for all values of p . However, it turns out that the main contribution to Γ_k comes from the values of p in the range $k < p < \tau$, and in this range one can do the following replacements: $1+n_r \simeq \tau/2\varepsilon_r$ and $1+n_s \simeq \tau/2\varepsilon_s$. Rather than going through the full justification, we simply assume that the replacement can be made, and we see that indeed the main contributions come from the momenta in the range $k < p < \tau$. This, in turn, justifies *a posteriori* the simplifications. The calculation now proceeds exactly as in B_1 . We will write the integrals only for the first term in M_{22} [Eq. (3.22)] for which the algebra is simpler. Once the integrations over the elliptical coordinates are done, we are left with an expression similar to Eq. (3.23) for the decay rate,

$$\Gamma_k^{(2)} = \frac{\omega_E \varepsilon_k \tau}{4\pi S^2} \int_{\lambda_2 k^3}^{\lambda_1 k^{1/3}} \frac{n_p p dp}{k+p} . \quad (3.29)$$

Let us change variables to $x = p/\tau$; the decay rate is then

$$\Gamma_k^{(2)} = \frac{\omega_E \varepsilon_k \tau^2}{4\pi S^2} \int_0^\infty \frac{x dx}{(x+k/\tau)(e^x-1)} , \quad (3.30)$$

which can easily be asymptotically evaluated as $k \ll \tau$,

$$\Gamma_k^{(2)} = \frac{\omega_E \varepsilon_k \tau^2}{4\pi S^2} \ln(\tau/k) . \quad (3.31)$$

As in B_1 , the evaluation of the last two terms in M_{22} [Eq. (3.22)] is more difficult, but can be done and leads to the same simple result, namely that they each contribute half as much as the first.

The contribution of *region 3* ($p > \lambda_1 k^{1/3}$) is negligible in this case because of the overall occupation factor n_p which is exponentially small. Therefore the expression of the decay rate for region B_2 is the same as that for region B_1 .

In sum, in the lowest Born approximation, for regime B' ($k \ll \tau$),

$$\Gamma_k = \frac{\omega_E \varepsilon_k \tau^2}{2\pi S^2} \ln(\tau/k) . \quad (3.32)$$

C. Regime C, $\tau \ll k \ll \tau^{1/3}$

In this regime, the reverse processes can be neglected ($1 - e^{-2\epsilon_k/\tau} \sim 1$). Again, we study the scattering contribution from three different ranges of incoming momentum p as defined in Eq. (3.15).

In *region 1* ($p < \lambda_2 k^3$), the calculation is exactly the same as in regime B_1 —region 1, but it comes from different approximations. The approximation in regime B_1 was

$$(1 - e^{-2\epsilon_k/\tau})(1 + n_r) \sim \frac{k}{\tau} \frac{\tau}{k} \sim 1;$$

now we have the same result with

$$((1 - e^{-2\epsilon_k/\tau})(1 + n_r)) \sim 1 \times 1 \sim 1.$$

The expression for the decay rate from this region is therefore the same as Eq. (3.19), which is smaller than the first-order contribution.

In *region 2* ($\lambda_2 k^3 < p < \lambda_1 k^{1/3}$), the major contribution to the integral is simply gotten if one replaces $1 + n_r$ and $1 + n_s$ by 1. In order to prove this, we simply need to bound the contributions of n_r and n_s in the integral; we will show this for the first term in M_{22} and give the result for the other two terms. We write the decay rate as

$$\Gamma_k = \frac{\omega_E}{8(2\pi)^3 S^2} \int d^2 p n_p (I_1 + 2I_2), \quad (3.33)$$

where I_1 corresponds to the contribution of the first in M_{22} [Eq. (3.22)] and I_2 corresponds to either the second or the third term in M_{22} , which give equal contributions. Specifically, let us look at the first term,

$$I_1 = \int d^2 q (1 + n_r)(1 + n_s) \frac{kp}{rs} (1 - \mu)^2 \delta(k + p - r - s), \quad (3.34)$$

with $\mu \equiv \hat{\mathbf{k}} \cdot \hat{\mathbf{p}}$. One gets an upper bound for the contribution of n_r and n_s by replacing them by a bigger quantity using the inequality $e^x - 1 \geq x$ for all $x \geq 0$. So we compute the integrals where we have replaced $1 + n_r \rightarrow 1 + \tau/r$ and $1 + n_s \rightarrow 1 + \tau/s$. We write

$$(1 + n_r)(1 + n_s) = 1 + n_r + n_s + n_r n_s, \quad (3.35)$$

and the contribution to I_1 is divided in three parts; $I_{1,a}$ corresponds to the first term in Eq. (3.35), $I_{1,b}$ corresponds to the second and third terms, and $I_{1,c}$ corresponds to the last term,

$$I_1 \equiv I_{1,a} + I_{1,b} + I_{1,c}. \quad (3.36)$$

We use the elliptical coordinates described in Eqs. (3.20) to perform the calculations, and we find

$$I_{1,a} \equiv kp(1 - \mu)^2 \int d^2 q \frac{\delta(k + p - r - s)}{rs}, \quad (3.37)$$

$$I_{1,b} = \pi \sqrt{2kp} (1 - \mu)^{3/2}; \quad (3.38)$$

likewise,

$$I_{1,b} \leq kp(1 - \mu)^2 \int d^2 q \frac{2\tau \delta(k + p - r - s)}{rs^2}, \quad (3.39)$$

$$I_{1,b} \leq 4\pi(1 - \mu)\tau \quad (3.40)$$

and

$$I_{1,c} \leq kp(1 - \mu)^2 \int d^2 q \frac{\tau^2 \delta(k + p - r - s)}{r^2 s^2}, \quad (3.41)$$

$$I_{1,c} \leq \frac{4\pi(1 - \mu)\tau^2}{p + k}. \quad (3.42)$$

At this stage, it is easy to perform exactly the p integrations to prove that indeed the contribution from $I_{1,a}$ is the largest. Alternatively, one can notice that since the contribution to the decay rate will come from thermal momenta, one needs only compare Eqs. (3.38), (3.40), and (3.42) when $p \sim \tau$.

For the second integral I_2 in Eq. (3.33), the same approximation can be made—we can neglect n_r and n_s compared to 1. All the integrals can then be evaluated exactly, and it turns out that

$$I_2 = \frac{3}{8} I_1. \quad (3.43)$$

This is different from regime B' where the second and the third terms in M_{22} yield just one half the contribution of the first.

The contribution of *region 3* ($p > \lambda_1 k^{1/3}$) is negligible because of the exponential in n_p . So, in regime C, the decay is mainly due to thermal magnons as is the case in 3D. The final result for the decay rate in regime C is

$$\Gamma_k = \frac{7\omega_E(\epsilon_k \tau^5)^{1/2}}{8(2\pi)^{3/2} S^2} \zeta(5/2). \quad (3.44)$$

D. Regime D, $\tau^{1/3} \ll \epsilon_k \ll 1$

In this regime, only region 1 ($p \ll k^3$) will contribute, because for the other values of p the exponential in n_p is very small. Here again we can replace $1 + n_r$ and $1 + n_s$ by 1. The expression for the decay rate is then

$$\Gamma_k = \frac{\omega_E}{2S^2(2\pi)^3} \int d^2 s d^2 p n_p (1 - \nu)(1 - \mu) \times \delta(p - s - v_k(p\mu - s\nu)). \quad (3.45)$$

The s and p integrations can be done as in regime B_1 , and one finds

$$\Gamma_k = \frac{3\omega_E \tau^3 \zeta(3)}{4\sqrt{2}\pi S^2 \sqrt{1 - v_k}} \quad (3.46)$$

or

$$\Gamma_k = \frac{3\omega_E \tau^3 \zeta(3)}{8\sqrt{2}\pi S^2 \epsilon_k \sqrt{f(\hat{\mathbf{k}})}}, \quad (3.47)$$

where f is defined by Eq. (2.24).

IV. SELF-CONSISTENCY OF THE BORN APPROXIMATIONS

In the foregoing calculation of the damping of long-wavelength magnons we have treated the intermediate

magnons as free particles, i.e., we have completely neglected their damping. To attain self-consistency, one must take into account the finite lifetime of all the magnons involved in the scattering process. Qualitatively, one may draw a distinction between the magnons whose inverse lifetime Γ_p is greater than the frequency of the incoming magnon $\omega_E \varepsilon_k$, and those for which Γ_p is smaller. One thus defines a cutoff momentum p_m such that

$$\Gamma_{p_m} \equiv \omega_E \varepsilon_k . \quad (4.1)$$

For the contribution to the damping coming from momenta p such that $p < p_m$, one would intuitively think that the calculation is already self-consistent, whereas for the momenta such that $p > p_m$, the situation is unclear. It is thus important to test the stability of the Born approximation with respect to the inclusion of damping in intermediate states.

We will show that the magnons with $p > p_m$ do not contribute to the leading order of Γ_k . It is interesting to note that this is contrary to what happens in three dimensions where HKHH have shown self-consistently that it is always the thermal magnons that dominate the scattering, even when $\tau > p_m$.

In fact, we also need to consider the stability of the Born approximation when the incoming magnon is not exactly on shell, i.e., when the condition $\omega = \omega_E \varepsilon_k$ is not satisfied. In this case the expression for the decay is more complicated than in Eq. (3.8); it must include the contribution of graphs that were identically zero for on-shell incoming magnons but that are different from zero for off-shell magnons as given in Eq. (2.16).

Let us define a reduced frequency $\tilde{\omega} = \omega / \omega_E$. The argument of the energy-conserving δ function becomes $\tilde{\omega} + \varepsilon_p - \varepsilon_r - \varepsilon_s$; for an off-shell incoming magnon $\tilde{\omega} \neq \varepsilon_k$. We must notice, for instance, that the expression for the matrix element M_{22} given in Eq. (3.22) is no longer valid because it used the fact that the incoming magnon was on shell.

We will now proceed and do the self-consistent analysis for off-shell magnons. The self-consistency condition will only affect the regimes where the important momenta p which give the main contribution to the decay are greater than the cutoff momentum p_m . This is not the case in re-

gimes *C* and *D* (where $\tau \ll \varepsilon_k$) because in these cases, the important momentum, the thermal momentum $p \sim \tau$, has a decay rate approximately given by

$$\Gamma_\tau \sim \omega_E \tau^3 / S^2 , \quad (4.2)$$

which is much smaller than the frequency of the incoming magnon,

$$\Gamma_\tau \ll \omega_E \tau \ll \omega_E \varepsilon_k . \quad (4.3)$$

On the other hand, when $\varepsilon_k \ll \tau$, we have seen that the dominant contributions come from a range of momenta $k < p < \tau$. In this regime Eq. (4.1) combined with Eq. (3.32) defines the cutoff momentum as

$$p_m \simeq 2\pi S^2 k / \tau^2 . \quad (4.4)$$

We have neglected the effect of the logarithm in Eq. (3.32) because it would only give a small logarithmic multiplicative correction to the definition of p_m which would in turn produce only a negligible additive correction to the self-consistent decay rate. It is clear that one should start to worry about self-consistency as soon as p_m becomes smaller than the upper end of the important interval, i.e., when $p_m < \tau$. This defines a new regime *A* ($p_m \ll \tau$) where we must do the calculation self-consistently,

$$\text{regime } A: k \ll \tau^3 / 2\pi S^2 . \quad (4.5)$$

Intuitively one may think that the only effect of self-consistency is to replace the upper end of the integral in Eq. (3.26) or (3.23) by p_m [in regime *A*, $p_m \ll (2\pi S^2 k)^{1/3}$] so that the logarithm in Eq. (3.28) gets transformed to

$$\ln(\tau/k) \rightarrow \ln(p_m/k) = \ln(2\pi S^2 / \tau^2) .$$

This is exactly what happens, as we are going to demonstrate.

First we must write the equivalent of Eq. (3.8) in the case of off-shell, self-consistent scattering. To this effect we follow HKHH and rewrite the mass operator with the fully dressed propagators in the intermediate states. From Eq. (4.12) in HKHH we have

$$\begin{aligned} \Gamma(k, \omega) &= \frac{\pi \omega_E (1 - e^{-2\tilde{\omega}/\tau})}{16S^2} \\ &\times \int \frac{d\tilde{\omega}_2}{2\pi} \int \frac{d\tilde{\omega}_3}{2\pi} \int \frac{d\tilde{\omega}_4}{2\pi} \int \frac{d^2 p}{(2\pi)^2} \int \frac{d^2 q}{(2\pi)^2} n(\tilde{\omega}_2) [1 + n(\tilde{\omega}_3)] [1 + n(\tilde{\omega}_4)] \tilde{A}(\mathbf{p}, \tilde{\omega}_2) \tilde{A}(\mathbf{s}, \tilde{\omega}_3) \tilde{A}(\mathbf{r}, \tilde{\omega}_4) \\ &\times [\delta(\tilde{\omega} + \tilde{\omega}_2 - \tilde{\omega}_3 - \tilde{\omega}_4) M_{22} + e^{2\tilde{\omega}/\tau} \delta(-\tilde{\omega} + \tilde{\omega}_2 - \tilde{\omega}_3 - \tilde{\omega}_4) M_{31}] , \end{aligned} \quad (4.6)$$

where $\tilde{\omega}_i = \omega_i / \omega_E$ and

$$\tilde{A}(k_i, \tilde{\omega}_i) = 2\hbar \omega_E \lim_{\eta \rightarrow 0^+} \text{Im} G_{\alpha, \alpha}(\mathbf{k}_i, \omega_i - i\eta) \quad (4.7)$$

is the spectral weight function. For undamped spin waves we have

$$\tilde{A}(\mathbf{k}_i, \tilde{\omega}_i) = 2\pi \delta(\tilde{\omega}_i - \varepsilon_i) , \quad (4.8)$$

in which case Eq. (4.6) reduces to Eq. (3.8).

In order to evaluate the decay rate we must solve Eq. (4.6) self-consistently, since the spectral weights are themselves functions of the mass operator Σ . Let us take $\tilde{A}(\mathbf{k}_i, \tilde{\omega}_i)$ to be a function sharply peaked about $\tilde{\omega}_i = \varepsilon_i$, whose dominant contribution occurs within a characteristic width γ_i which is assumed to be of order $k_i \tau^2 / S^2$. In particular, we are assuming here that any collective effects of the magnon interactions such as possible bound states or ‘‘second magnons’’ may be neglected in the spectral weight function at long wavelengths. If we now perform the $\tilde{\omega}_i$ integrations in Eq. (4.6), we may replace the frequencies $\tilde{\omega}_i$ in the occupation numbers by the corresponding energies ε_i , since the occupation numbers vary on a scale $\tau \gg \gamma_i$. The integrations over frequency then reduce to

$$\int \frac{d\tilde{\omega}_2}{2\pi} \int \frac{d\tilde{\omega}_3}{2\pi} \int \frac{d\tilde{\omega}_4}{2\pi} \tilde{A}(\mathbf{p}, \tilde{\omega}_2) \tilde{A}(\mathbf{s}, \tilde{\omega}_3) \tilde{A}(\mathbf{r}, \tilde{\omega}_4) \delta(\tilde{\omega} + \tilde{\omega}_2 - \tilde{\omega}_3 - \tilde{\omega}_4) \equiv \phi(\tilde{\omega} + \varepsilon_p - \varepsilon_s - \varepsilon_r), \quad (4.9)$$

where the function $\phi(x)$ is sharply peaked at $x = 0$, with a width γ equal to the sum of the widths γ_i ,

$$\gamma \sim (p + r + s) \tau^2 / S^2,$$

and $\phi(x)$ obeys the approximate sum rule

$$\int_{-\infty}^{+\infty} \phi(x) dx \approx 1. \quad (4.10)$$

This sum rule is exact when the fluctuations tend to zero (i.e., when $S \rightarrow \infty$ and $T \rightarrow 0$); at finite S , we believe that the effect of the fluctuations can be incorporated by using the right long-wavelength parameters for the expression of the damping as stated in the Introduction. Let us define ρ as the ratio of the frequency of the incoming magnon to the equivalent on-shell magnon: $\tilde{\omega} \equiv \rho \varepsilon_k$. We can now write (4.6) in the form

$$\Gamma(k, \omega) = \frac{\pi \omega_E \rho k}{16 S^2 (2\pi)^4 \tau} \int d^2 p d^2 q d\alpha n_p (1 + n_r) (1 + n_s) \phi(\alpha) \times [\delta(\rho \varepsilon_k + \varepsilon_p - \varepsilon_r - \varepsilon_s - \alpha) M_{22} + \delta(-\rho \varepsilon_k + \varepsilon_p - \varepsilon_r - \varepsilon_s - \alpha) M_{31}]. \quad (4.11)$$

In regime *A* we need only worry about the contribution coming from momenta p such that $k < p < \tau$, but this contribution will come in two parts, one where the scattering surface is approximately an ellipse and one where the scattering surface comprises two disjoint parts. We will compute separately the effect of self-consistency in the two cases. From the definition of regime *A*, one can see that (at least if S is not too large) the cutoff momentum p_m falls into the region where the scattering surface is elliptical, since $p_m \ll (2\pi S^2 k)^{1/3}$. Therefore we expect the second region not to contribute to the leading term as a consequence of taking into account the lifetime of intermediate magnons.

Let us first examine the elliptical region, $\lambda_2 k^3 < p < \lambda_1 k^{1/3}$. We can expand the exponentials to get

$$\Gamma(k, \omega) = \frac{\pi \omega_E \rho k \tau^2}{16 S^2 (2\pi)^4} \int d^2 p d\alpha \frac{\phi(\alpha)}{p} \int \frac{d^2 q}{rs} [\delta(\rho \varepsilon_k + \varepsilon_p - \varepsilon_r - \varepsilon_s - \alpha) M_{22} + \delta(-\rho \varepsilon_k + \varepsilon_p - \varepsilon_r - \varepsilon_s - \alpha) M_{31}], \quad (4.12)$$

where we can write the matrix elements in the long-wavelength limit as in Eqs. (2.18) and (2.19). Let us define the integrations over the elliptical surface coming, respectively, from the matrix elements M_{22} and M_{31} to be I_a and I_b :

$$\Gamma(k, \omega) = \frac{\pi \omega_E \rho k \tau^2}{16 S^2 (2\pi)^4} \int d^2 p d\alpha \frac{\phi(\alpha)}{p} [I_a + I_b]. \quad (4.13)$$

Then we use the elliptical coordinates introduced in Eq. (3.20) to write the integral I_a ,

$$I_a \equiv \int \frac{d^2 q}{rs} \delta(\rho \varepsilon_k + \varepsilon_p - \varepsilon_r - \varepsilon_s - \alpha) M_{22}, \quad (4.14)$$

in terms of the variables u and v as

$$I_a = 2 \int du dv \delta(2g_1 - 2c \cosh u) M_{22}, \quad (4.15)$$

where $g_1 \equiv \rho \varepsilon_k + \varepsilon_p - \alpha$. We must express the matrix element M_{22} in terms of u and v . To do that, we write

$$\hat{\mathbf{r}} = \frac{(1 - \cosh u \cos v) \hat{\mathbf{x}} - \sinh u \sin v \hat{\mathbf{y}}}{\cosh u - \cos v} \quad (4.16)$$

and

$$\hat{\mathbf{s}} = \frac{(1 + \cosh u \cos v) \hat{\mathbf{x}} + \sinh u \sin v \hat{\mathbf{y}}}{\cosh u + \cos v}. \quad (4.17)$$

We must also introduce the following notations: $\hat{\mathbf{k}} \cdot \hat{\mathbf{p}} = \mu$, $\hat{\mathbf{k}} \cdot \hat{\mathbf{x}} = \gamma$, $\hat{\mathbf{k}} \cdot \hat{\mathbf{y}} = \bar{\gamma}$, $\hat{\mathbf{p}} \cdot \hat{\mathbf{x}} = \beta$, $\hat{\mathbf{p}} \cdot \hat{\mathbf{y}} = \bar{\beta}$, where, as before, $\hat{\mathbf{x}} = \hat{\mathbf{c}}$. The u and v integrations can be done exactly and yield

$$I_a = \frac{8\pi}{c \sinh^2 u_0 \cosh u_0} [(1-\mu) \sinh^2 u_0 + (\cosh u_0 - \gamma)(\cosh u_0 - \beta) \\ + (1-\gamma \cosh u_0)(\beta \cosh u_0 - 1) \cosh u_0 (\cosh u_0 - \sinh u_0) - \bar{\gamma} \bar{\beta} \sinh^3 u_0 (\cosh u_0 - \sinh u_0)] , \quad (4.18)$$

where u_0 is defined by $\cosh u_0 = g_1/c$. Since the major contribution only comes from $k < p < \lambda_1 k^{1/3}$, we can expand I_a to lowest order in k/p , otherwise the p integration is too difficult to do. To lowest order the result is simple and

$$I_a = \frac{32\pi(1-\mu)}{p} \Theta(k(\rho-\mu)-2\alpha) , \quad (4.19)$$

where the Θ function is equal to 1 when its argument is positive and 0 otherwise and expresses the condition that $g_1/c \geq 1$, i.e., $k(\rho-\mu)-2\alpha \geq 0$.

The same manipulation can be performed for I_b with the result that

$$I_b = \frac{-32\pi(1+\mu)}{p} \Theta(-k(\rho+\mu)-2\alpha) , \quad (4.20)$$

which enters when $g_2 \equiv -\rho k/2 + p/2 - \alpha \geq c$; i.e., $k(\rho+\mu)+2\alpha \leq 0$.

Putting this back into Eq. (4.13) we find that

$$\Gamma(k, \omega) = \frac{\pi \omega_E \rho k \tau^2}{S^2 (2\pi)^3} \int \frac{d^2 p (1-\mu)}{p^2} \int d\alpha \phi(\alpha) [\Theta(k(\rho-\mu)-2\alpha) - \Theta(-k(\rho-\mu)-2\alpha)] . \quad (4.21)$$

At this point, we can approximate the contribution of the momenta $p > p_m$ and show that it is negligible to first order. For the values of p such that $\gamma \gg k$, i.e., $p \gg p_m$, then the α integral is going to be approximately equal to

$$\int d\alpha \phi(\alpha) [\Theta(k(\rho-\mu)-2\alpha) - \Theta(-k(\rho-\mu)-2\alpha)] \propto k/\gamma \propto k S^2 / p \tau^2 , \quad (4.22)$$

provided that we assume that the function ϕ is slowly varying on frequency scales much smaller than γ . Let us now compute the contribution of the range $p_m < p < \lambda_1 k^{1/3}$,

$$\Gamma(k, \omega) \sim \frac{\pi \omega_E \rho k \tau^2}{S^2 (2\pi)^3} \int_{p_m}^{\lambda_1 k^{1/3}} \frac{d^2 p (1-\mu) k S^2}{p^3 \tau^2} , \quad (4.23)$$

$$\Gamma(k, \omega) \sim \frac{\omega_E k^2}{p_m} \sim \frac{\omega_E k \tau^2}{S^2} . \quad (4.24)$$

This value is asymptotically negligible compared to the first-order contribution.

By contrast, for the values of p such that $\gamma \ll k$, i.e., $p \ll p_m$, then the integral becomes

$$\int d\alpha \phi(\alpha) [\Theta(k(\rho-\mu)-2\alpha) - \Theta(-k(\rho-\mu)-2\alpha)] \sim 1 , \quad (4.25)$$

because most of the weight of $\phi(x)$ corresponds to values of x of order γ . In this case, the expression for the decay rate is the same as in regime B' , with the only difference that the upper limit of the integral is changed from being $\lambda_1 k^{1/3}$ in regime B' to being p_m in the self-consistent calculation. Equation (4.21) can be written as

$$\Gamma(k, \omega) = \frac{\pi \omega_E \rho k \tau^2}{S^2 (2\pi)^2} \int_k^{p_m} \frac{dp}{p} , \quad (4.26)$$

which yields for the self-consistent regime:

$$\Gamma(k, \omega) = \frac{\rho \omega_E \epsilon_k \tau^2}{2\pi S^2} \ln(2\pi S^2 / \tau^2) . \quad (4.27)$$

As promised, the only effect of introducing self-consistency is to diminish the scattering by the magnons which are not well defined at an energy scale of order ϵ_k . It is also apparent in Eq. (4.27) that the only effect of considering off-shell magnons is to replace ω_k by ω (i.e., $\omega_E \epsilon_k \rightarrow \rho \omega_E \epsilon_k$) in the expression of the decay rate so that we recover the on-shell result trivially when $\rho = 1$.

We must now investigate the contribution from the region $\lambda_1 k^{1/3} < p < \tau$. As in regime B' , we know that the major contribution will come from replacing $1+n_r$ and $1+n_s$ by $1+n_p$ and τ/s , respectively. Also, we can still integrate over one of the two disjoint surfaces and multiply this contribution by 2. We choose the surface such that $p \sim r \gg k, s$. For this choice, the matrix elements given by Eqs. (2.18) and (2.19) have simple expressions,

$$M_{22} = 4(1-\mu)(1-\nu) , \quad (4.28)$$

$$M_{31} = 4(1+\mu)(1-\nu) , \quad (4.29)$$

where $\mu \equiv \hat{v}_p \cdot \hat{\mathbf{k}}$ and $\nu \equiv \hat{v}_p \cdot \hat{\mathbf{s}}$. We can write Eq. (4.11) for the decay as

$$\Gamma(k, \omega) = \frac{\omega_E \rho k}{S^2 (2\pi)^3} \int_{s \sim 0} d^2 p d^2 s d\alpha n_p (1+n_p) \frac{\phi(\alpha)(1-\nu)}{s} \\ \times [\delta(\rho k + v_p s \nu - v_p k \mu - s - \alpha)(1-\mu) - \delta(-\rho k + v_p s \nu - v_p k \mu - s - \alpha)(1+\mu)]. \quad (4.30)$$

In the term corresponding to the second matrix element we make the change of variable $\mu \rightarrow -\mu$ and we use the α integral to satisfy the δ functions,

$$\Gamma(k, \omega) = \frac{\omega_E \rho k}{S^2 (2\pi)^3} \int_{s \sim 0} d^2 p d^2 s n_p (1+n_p) \frac{\phi(\alpha)(1-\nu)(1-\mu)}{s} [\phi(\rho k + v_p s \nu - v_p k \mu - s) - \phi(-\rho k + v_p s \nu + v_p k \mu - s)]. \quad (4.31)$$

Since in this regime k is very small compared to γ , we can do a Taylor series expansion for $\phi(x)$ and write

$$\Gamma(k, \omega) = \frac{2\omega_E \rho k}{S^2 (2\pi)^3} \int_{s \sim 0} d^2 p d^2 s n_p (1+n_p) \frac{(1-\nu)(1-\mu)}{s} (\rho - \mu) k \phi'((\nu-1)s), \quad (4.32)$$

where we have replaced v_p by one. The s integration is then easy to do and

$$\Gamma(k, \omega) = \frac{2\omega_E \rho k^2}{S^2 (2\pi)^2} \int d^2 p n_p (1+n_p) \phi(0)(1-\mu)(\rho - \mu), \quad (4.33)$$

and for a reasonable weight function ϕ , we must have $\phi(0) \propto 1/\gamma$ so that we can get an estimate of the contribution of this term:

$$\Gamma(k, \omega) \propto \frac{\omega_E k^2}{\tau}. \quad (4.34)$$

We are in a regime where $k \ll \tau^3/2\pi S^2$, so Eq. (4.34) gives

$$\Gamma(k, \omega) \lesssim \frac{\omega_E k \tau^2}{S^2}, \quad (4.35)$$

which is, as promised, smaller than the leading term with the logarithm given by Eq. (4.27).

If we now introduce a lower bound $k_{\min}(T)$, as yet to be specified, for the validity of regime *A*, we can summarize the results obtained so far as follows:

regime *A* [$k_{\min}(\tau) \ll k \ll \tau^3/2\pi S^2 \ll 1$]:

$$\Gamma_k = \frac{\omega_E \epsilon_k \tau^2}{2\pi S^2} [\ln(2\pi S^2/\tau^2) + u_A], \quad (4.36)$$

regime *B* ($\tau^3/2\pi S^2 \ll k \ll \tau \ll 1$):

$$\Gamma_k = \frac{\omega_E \epsilon_k \tau^2}{2\pi S^2} [\ln(\tau/k) + u_B], \quad (4.37)$$

regime *C* ($\tau \ll k \ll \tau^{1/3} \ll 1$):

$$\Gamma_k = \frac{7\omega_E (\epsilon_k \tau^5)^{1/2}}{8(2\pi)^{3/2} S^2} \zeta(5/2), \quad (4.38)$$

regime *D* ($\tau^{1/3} \ll k \ll 1$):

$$\Gamma_k = \frac{3\omega_E \tau^3 \zeta(3)}{8\sqrt{2}\pi S^2 \epsilon_k \sqrt{f(\hat{\mathbf{k}})}}. \quad (4.39)$$

In regimes *A* and *B* the first correction to the logarithmic term is a constant, which should be of order one. In order to restore the dimensions of the wave vectors, one should replace, in the equations given above, k by $\sqrt{2}ka$, where a is the lattice constant of the original QHAF. Also, to make contact with the results as quoted in the Introduction, Eqs. (1.1)–(1.4), one should express the results in terms of the physically relevant parameters, the spin-stiffness constant ρ_S and the spin-wave velocity c . In the large- S limit, one writes

$$\rho_S = JS^2 \quad (4.40)$$

and

$$c = \frac{\sqrt{8}JSa}{\hbar}. \quad (4.41)$$

Once these replacements are made, one gets the formulas quoted in the Introduction.

V. DAMPING OF SPIN WAVES IN THE CLASSICAL REGIME

A. Large- S limit

One can obtain the classical Heisenberg antiferromagnet from the QHAF by taking the following limits:

$$\hbar \rightarrow 0, \quad J \rightarrow 0, \quad S \rightarrow \infty,$$

while holding the spin stiffness and the spin-wave velocity constant:

$$\rho_0 = JS^2, \quad (5.1)$$

$$c_0 = \frac{\sqrt{8}JSa}{\hbar}. \quad (5.2)$$

In this limit the Bose occupation numbers for the classical low-temperature regime become arbitrarily large since $\tau = TS/2\rho_0$ is going to infinity,

$$n_p \sim TS/4\varepsilon_p \rho_0 \rightarrow \infty .$$

In order to get rid of that divergence, we define the classical operators:

$$\tilde{\alpha}_p = S^{-1/2} \alpha_p, \quad \tilde{\beta}_p = S^{-1/2} \beta_p ,$$

with finite occupation number

$$\tilde{n}_p = T/4\varepsilon_p \rho_0 .$$

We can then write the Hamiltonian as in the quantum case, the perturbation expansion is the same, and we obtain an expression for the decay equivalent to Eq. (2.16) (see Ref. 6 for details)

$$\begin{aligned} \Gamma_k &= \frac{\pi\sqrt{2}c_0\varepsilon_k^2}{(16N)^2\alpha} (T/\rho_0)^2 \\ &\times \sum_{\mathbf{p}, \mathbf{s}} \frac{1}{\varepsilon_k \varepsilon_p \varepsilon_r \varepsilon_s} \delta(\varepsilon_k + \varepsilon_p - \varepsilon_r - \varepsilon_s) M_{22}(\mathbf{k}, \mathbf{p}, \mathbf{r}, \mathbf{s}) . \end{aligned} \quad (5.3)$$

The computation of the on-shell decay rate in the Born approximation is almost exactly the same as for regimes B_1 and B_2 . The only difference is that the sums are not cut off by the exponential decay of the occupation factors. So, in principle, we should integrate out to the edge of the Brillouin zone. Since the upper cutoff comes in a logarithm, we can choose any finite upper cutoff that we want and correct for it in the unknown constant term. The result is similar to Eqs. (4.36) and (4.37):

$$\Gamma_k = \frac{c_0 k}{8\pi} (T/\rho_0)^2 [\ln(1/ka) + \text{const}] , \quad (5.4)$$

where the constant is *a priori* different.

The result of the first Born approximation is altered by the self-consistency condition exactly in the same manner as in Sec. IV. We define a cutoff momentum p_m as in Eq. (4.1) and we find for p_m ,

$$p_m = 8\pi k (\rho_S/T)^2 , \quad (5.5)$$

as in Eq. (4.4).

Therefore, the classical case is split in two regimes depending on whether p_m is greater or smaller than the zone edge. In the first regime, the self-consistency condition cuts off the contribution of the zone edge and we have a long-wavelength expression for Γ_k independent of the short-wavelength cutoff and identical to quantum regime A :

regime A_{cl} [$k_{\min} a \ll ka \ll (T/\rho_S)^2/8\pi$]:

$$\Gamma_k = \frac{\pi ck}{2} \left[\frac{T}{2\pi\rho_S} \right]^2 [2 \ln(2\pi\rho_S/T) + \text{const}] , \quad (5.6)$$

where the constant is the same as in quantum regime A in Eq. (1.1), $\text{const} = \ln(2/\pi) + u_A$, as we shall see below.

The second regime is defined as follows:

regime B_{cl} [$(T/\rho_S)^2/8\pi \ll ka \ll 1$]:

$$\Gamma_k = \frac{\pi ck}{2} \left[\frac{T}{2\pi\rho_S} \right]^2 [\ln(1/ka) + \text{const}] , \quad (5.7)$$

where, *a priori*, the constant is different from quantum regime B in Eq. (1.2). However, we can estimate it if we use the mapping of the QHAF onto the CLRM as will be shown shortly.

The formulas for the damping must be the same in regimes A and A_{cl} because the integrals for the damping are essentially the same. Suppose that the value of k is near the upper bound of the region A or A_{cl} . Then the wave vectors p that are most important for the intermediate magnon will be in the regime B or B_{cl} . The damping Γ_p of the intermediate magnon is the same in the two cases (assuming that T/ρ_S and c are chosen to be the same) except for a difference in the arguments of the logarithm and the additive constants which appear in the brackets as the final factors of Eqs. (5.7) and (1.2). However, the damping at wave vector k depends only logarithmically on Γ_p , so the difference between the formulas (5.7) and (1.2) will be negligible in the limit of interest, where $(T/\rho_S) \rightarrow 0$. By iteration of the above arguments, we see that Γ_k becomes even less sensitive to the difference between the classical and quantum cases if k is sufficiently small that the intermediate magnon p is itself in the wave vector region of A or A_{cl} .

B. Mapping between the classical and quantum systems

Although we have not attempted to calculate the constant after the logarithm in Eq. (5.7), it is possible to make an educated guess or estimate its magnitude, based on previous experience. CHN have discussed in detail the correspondence between the short-wavelength cutoff of the renormalization-group equations for the spin-stiffness constant $\rho_S(k, T)$ in the quantum Heisenberg antiferromagnet and the classical Heisenberg system. (For the static quantity, it does not matter whether the classical system is a ferromagnet, antiferromagnet, or CLRM.) They found that formulas in the two cases become identical if the lattice constant a of the classical model is replaced, in the QHAF, by the temperature-dependent quantity

$$a_{\text{eff}} = \sqrt{32} e^{\pi/2} (\hbar c/T) . \quad (5.8)$$

Note the large numerical factor ($\sqrt{32} e^{\pi/2} \approx 27.2$), which was also found previously by Parisi¹⁴ in the transformation between the lattice cutoff and the Pauli-Villars regularization of the 2D nonlinear sigma model. One effect of this large factor is that when expressed in terms of the variable $(T/2\pi\rho_S)$, the formula for the correlation length ξ in the classical model contains a coefficient of order 0.01, as was first noted by Shenker and Tobochnik,¹⁵ whereas the expression in the QHAF contains a coefficient of order unity. Specifically the formula obtained by CHN for the spin- $\frac{1}{2}$ QHAF was

$$\xi \approx 0.5a \frac{\exp(2\pi\rho_S/T)}{1 + (T/2\pi\rho_S)} , \quad (5.9)$$

while in the classical model, one has

$$\xi \approx 0.01a \frac{\exp(2\pi\rho_S/T)}{(2\pi\rho_S/T) + 1} . \quad (5.10)$$

The integrals which enter the spin-wave damping in the regime B_{cl} are not identical to the integrals which were evaluated to obtain the conversion factor for the renormalization of ρ_S . Nevertheless there is a certain similarity in the physics; because the frequencies of the zone-boundary magnons or vibrational modes are considerably smaller than one would guess by a linear extrapolation of the spectrum at small k , the short-wavelength fluctuations are considerably enhanced. Therefore, the effects of these fluctuations in reducing the value of ρ_S , or in scattering magnons of longer wavelength, should be significantly larger than one would expect by simply using a Debye approximation where the linear spectrum is cut off abruptly at the boundary of the Brillouin zone, i.e., by setting $p_{max} = \sqrt{2\pi}a^{-1}$ for the classical antiferromagnet or $p_{max} = 2\sqrt{\pi}a^{-1}$ for the CLRM. By contrast, the quantum mechanical cutoff which occurs when the magnon frequency exceeds T/\hbar is rather well approximated by a simple truncation at $p_{max} = T/\hbar c$.

In this spirit, we may write the spin-wave damping in the various regimes as follows:

regime A or A_{cl} :

$$\Gamma_k = \frac{\pi ck}{2} \left[\frac{T}{2\pi\rho_S} \right]^2 [2 \ln(2\pi\rho_S/T) + \ln(2/\pi) + u_A], \quad (5.11)$$

regime B :

$$\Gamma_k = \frac{\pi ck}{2} \left[\frac{T}{2\pi\rho_S} \right]^2 [\ln(T/\hbar ck) + u_B], \quad (5.12)$$

regime B_{cl} :

$$\Gamma_k = \frac{\pi ck}{2} \left[\frac{T}{2\pi\rho_S} \right]^2 [\ln(1/ka) + \ln(\sqrt{32}e^{\pi/2}) + u_{B_{cl}}], \quad (5.13)$$

where u_A , u_B , and $u_{B_{cl}}$ are constants that we assume small.

It is also convenient to slightly revise the definition of the crossover point $k_{AB}^{(cl)}$ between regimes A_{cl} and B_{cl} . If we require the expressions (5.11) and (5.13) for Γ_k be equal at $k_{AB}^{(cl)}$, we find

$$k_{AB}^{(cl)} = \frac{1}{a} \left[\frac{T}{2\pi\rho_S} \right]^2 \sqrt{8\pi} e^{\pi/2} \exp(u_{B_{cl}} - u_A). \quad (5.14)$$

In Sec. VI, when we compare our results with simulations on the CLRM, we shall treat u_A and $u_{B_{cl}}$ as adjustable parameters, and assume a sharp crossover from Eq. (5.11) to Eq. (5.13) at $k_{AB}^{(cl)}$.

C. Remarks on the classical lattice rotor model

In the present paper, we have not performed an explicit microscopic calculation of the damping of excitations in the CLRM, nor have we introduced the formalism appropriate for such a calculation. It is clear, however, as discussed in CHN, that the properties of the CLRM and

the classical Heisenberg antiferromagnet at wavelengths long compared to the lattice constant are identical in the limit $T \rightarrow 0$. The symmetries and excitation spectra are the same, and the interactions between the long-wavelength excitations are physically determined by geometric considerations which are identical in the two models.^{16,17} Moreover, the static equilibrium statistical properties of the CLRM and classical Heisenberg antiferromagnet are equivalent at *all* wave vectors.

As a consequence of these considerations, we expect that the damping in regime A_{cl} , at low temperatures and long wavelengths, should be identical in the CLRM and the Heisenberg model. In region B_{cl} , where the intermediate excitations responsible for damping extend to wave vectors close to the zone boundary, there may be a slight difference between the two systems. In particular, the small constant $u_{B_{cl}}$ which enters Eq. (5.13) may be different in the CLRM and the classical Heisenberg model.

D. Renormalization due to thermal excitations

As was discussed in the Introduction, the effective spin-stiffness constant ρ_S and the excitation frequency ck are strongly renormalized at very long wavelengths in the two-dimensional Heisenberg systems, quantum or classical, because of the infrared divergence arising from thermal excitations.

The simplest way to take these effects, at least approximately, into account, is to simply replace ck in the formulas for Γ_k by the actual frequency $\omega_k(T)$, and to replace ρ_S by the function $\rho_S(k, T)$ given by Eq. (1.7). To test the consistency of this assumption, we may return to the basic integral for Γ_k in regime A or A_{cl} , and ask what happens if we take into account the renormalization of the spin stiffness and frequencies of the intermediate state magnons responsible for the damping. The fluctuation reduction of the spin stiffness will lead to an increase in the occupation numbers and an enhancement of the scattering which will depend, in principle, on the wave vectors \mathbf{p} , \mathbf{r} , and \mathbf{s} , and therefore will change the form of the integrand. (There are also changes in the matrix element, resulting from the change in ρ_S , which must also be included.) However, in the limit of $T \rightarrow 0$, if $k\xi$ is fixed but very large, one finds that the value of $\rho_S(p, T)$ for the contributing intermediate states is not very different from the value of $\rho_S(k, T)$. In this regime, then, the value of the integral is simply obtained by replacing ρ_S by $\rho_S(k, T)$ in the final result. By contrast, the replacement is not well justified if the temperature is too high, or if one goes to wave vectors which are too small ($k\xi \approx 1$).

VI. NUMERICAL SIMULATIONS

CHN have argued that the dynamic properties of the Heisenberg antiferromagnet at sufficiently low temperatures and frequencies, and wave vectors close to the antiferromagnetic Bragg peak, may be related directly to the low-frequency long-wavelength behavior of a *classical* lattice rotor model (CLRM) [defined by Eq. (6.1) below],

which can be studied by molecular dynamics simulations.

In this section we will first describe the simulations of the CLRM and discuss their reliability in different regimes. Then we will compare the results of the simulations with the expressions for the damping in the classical case including the renormalization due to finite temperatures.

We now present the results of a molecular dynamics simulation of the CLRM. To that effect let us first describe the equations and the parameters of the CLRM. The model is described by a classical Lagrangian of the form

$$L = \frac{I}{2} \sum_i |\dot{\Omega}_i|^2 + \frac{K}{a^{2-d}} \sum_{\langle i,j \rangle} \Omega_i \cdot \Omega_j, \quad (6.1)$$

where $\{\Omega_i\}$ are a set of three-dimensional unit vectors, representing the orientations of the rotors associated with the sites $\{i\}$ of a 2D square lattice with lattice constant a , and the second sum is over nearest-neighbor pairs $\langle i,j \rangle$. The coefficient K is a stiffness constant which we may identify with the constant ρ_s , while the moment of inertia I of the rotors is related to the perpendicular susceptibility χ_\perp^0 by $\chi_\perp^0 \equiv I a^{-d}$. Each site represents a rotor which can be thought of as a point mass constrained to stay on the surface of a unit three-dimensional sphere. The interaction between neighbors is such that they want to be aligned.

In order to obtain a canonical ensemble we couple the system to a heat bath, which introduces a random force and a damping on each rotor. The equations of motion are then Langevin equations:

$$\begin{aligned} \Omega_i \times \ddot{\Omega}_i = & -\frac{K}{I a^{2-d}} \Omega_i \times \sum_j' (\Omega_i - \Omega_j) - \gamma \Omega_i \times \dot{\Omega}_i \\ & + \Omega_i \times \eta_i(t), \end{aligned} \quad (6.2)$$

where γ is the coupling constant to the heat bath, the sum is restricted to nearest neighbors of i , and the random force η_i obeys

$$\langle \eta_i^\alpha(t) \eta_j^\beta(t') \rangle = 2\gamma T \delta_{ij} \delta(t-t') \delta_{\alpha\beta}. \quad (6.3)$$

We use units such that $K=1$, $I=1$, and $a=1$. In these units, the zone-edge magnon has a frequency $\omega=2\sqrt{2}$. In order to integrate the equations of motion, we use a modified version of the algorithm used by Morf and Stoll:¹⁸

$$\begin{aligned} \Omega(t+\Delta) = & \Omega_0(t+\Delta) + (e^{-\gamma\Delta} - 1)[\Omega_0(t+\Delta) - \Omega(t)] \\ & - \Delta^2 e^{(-\gamma\Delta/2)} \bar{F}(t) + \mathcal{O}(\Delta^3), \end{aligned} \quad (6.4)$$

where $\Omega_0(t+\Delta)$ is the position the rotor would have at time $t+\Delta$ if there were no forces and no friction. The force $\bar{F}(t)$ is the combination of the forces derived from the Hamiltonian computed at time t and a random force which represents η_i .

At the beginning of the program the rotors start from a random position with zero initial velocity and are strongly coupled to the heat bath ($\gamma=1$) for 1200 iterations; the coupling is then gradually reduced to zero. We then keep the damping equal to zero and let the system evolve free-

ly. The data are recorded only when the sample evolves freely. In order to conserve energy along the run, we choose a small time step for integrating the equations of motion ($\Delta t=0.02$). The total energy is well conserved, indeed, for a run of total time $t \approx 2600$, the energy lost is only about 1.5%; this induces a systematic variation of temperature which is smaller than the statistical fluctuations due to the finiteness of the sample. Along with energy, in the absence of external damping, the total angular momentum of the system is also conserved:

$$L = \sum_i \Omega_i \times \dot{\Omega}_i. \quad (6.5)$$

This represents an overall rotation of the system at a rate $\omega_r = L/N$, where N is the number of rotors. At low temperatures this frequency scales as

$$\omega_r \propto \sqrt{T/N}, \quad (6.6)$$

which rapidly becomes greater—as the temperature goes to zero—than the width that we are trying to observe ($\Gamma_k \propto T^2$). For this reason we actually perform our measurements in a rotating frame where $L=0$. Namely, before recording the positions of the rotors at time t , we operate on them with a rotation of angle $-\omega_r t$ about the axis defined by L . This eliminates some spurious widening of the spin-wave peaks at low temperatures and long wavelengths.

For a given run, after every interval of time of $t_0 \approx 2.5$, the positions of the rotors are rotated, Fourier transformed in space, and stored. At the end of the run they are Fourier transformed in time, and we can compute the correlation functions $S(k, \omega)$,

$$S(k, \omega) \equiv \langle |\Omega(k, \omega)|^2 \rangle. \quad (6.7)$$

$S(k, \omega)$ is calculated for runs which corresponds to 2^{17} time steps, or a total time $t \approx 2621$. At the end of a run a configuration of the system is preserved and is then used as the seed of the next run. At equilibrium, positions and velocities are independent; hence a new thermalized sample is obtained by starting from the positions at the end of the previous run and giving the rotors a set of new velocities according to a two-dimensional Maxwellian distribution at the given temperature. At each temperature ten runs are made and the quantities of interest are averaged.

We then extract the location ω_k and width γ_k of the spin-wave peaks by fitting the sum of two Lorentzians to the dynamic-correlation function,

$$S(k, \omega) = \frac{P\gamma_k}{(\omega - \omega_k)^2 + \gamma_k^2} + \frac{P\gamma_k}{(\omega + \omega_k)^2 + \gamma_k^2}, \quad (6.8)$$

where P is a normalization constant and P , ω_k , and γ_k are fitting parameters. The fit is performed by minimizing the χ^2 ; we weight the region of the spin-wave peaks much more than the tails.

The assumption of Lorentzian line shapes is justified theoretically when the magnon damping is small, so that the peaks are well separated, and we are looking at frequencies that are not too far from one of the magnon peaks. For ω far from ω_k , or when the magnon peaks overlap strongly, Eq. (6.8) is merely a convenient form

which has a minimum number of adjustable parameters, but cannot be justified theoretically. Indeed, it appears from our numerical simulations that in the intermediate damping regime there is more weight at small frequencies than predicted by (6.8), but we have not attempted a systematic analysis of this point.

We have made runs at very low temperatures (down to $T=0.179$) where the correlation length is vastly greater than the system size [$\xi(T=0.179) \approx 5 \times 10^{11}$]. This is not, by itself, a problem for the validity of our calculations because, when $k\xi$ is large, there is no contribution to the integral for Γ_k from intermediate wave vectors p of order ξ^{-1} . In fact, the important values of p are large compared to k , when k and τ become small. Eventually, however, when the damping of the intermediate magnons is sufficiently small, it will become necessary in a finite system to replace the integral over intermediate states by a sum, and finite size complications will then set in.

In order to test the size dependence of our simulations, we have performed the measurements on different size lattices (64×64 , 128×128 , and 256×256). When the size was increased, the spin-wave peaks became narrower at long wavelengths and were little affected at short wavelengths. For instance, going from 64 to 128 at a temperature $T \approx 0.29$ gave peaks about 20–30% narrower at wave vector $k=0.1$ and about 5–10% narrower at $k=0.5$.

The smallest frequency that we can measure is

$$\omega_m = 2\pi/T \approx 0.0024, \quad (6.9)$$

which is of the order of the smallest widths that we obtain from the fit. The widths of the order of ω_m must be taken with caution. At the lower temperatures—where the lack of LRO is insignificant—the fact that some of our data seem not to tend to zero as k goes to zero is not significant and may be an artifact of the lack of precision both due to the finite size of the lattice and the finite run time. Another issue is that, for the values of the wave vector k small enough that the spin-wave peaks are not well separated, the precise form of the fitting function becomes important. The form that we have chosen, i.e., the sum of two Lorentzians, presents two distinct peaks as soon as $\omega_k > \gamma_k/\sqrt{3}$; by contrast, if we had chosen the product of two Lorentzians instead, we would have two distinct peaks only when $\omega_k > \gamma_k$. The widths thus extracted would be sensibly different. However, this only concerns the smallest wave vectors at our highest temperatures; at the lower temperatures ($T \lesssim 0.6$), the spin-wave peaks are well separated for the smallest value of k measured, other than $k=0$, which we exclude from our analysis.

Let us now compare the widths extracted from the fit with the expressions for the damping in the classical case given by Eqs. (5.11) and (5.13). As discussed above, we use Eq. (1.7) evaluated at k for the renormalized value of ρ_S in both regimes. We should also use a scaling form for the velocity c , but the renormalized spin-wave frequency ω_k is also extracted from the fit and we use this value in the formulas. There are two adjustable parameters in the formulas, the constants u_A and $u_{B_{cl}}$. In Fig. 1 we plot

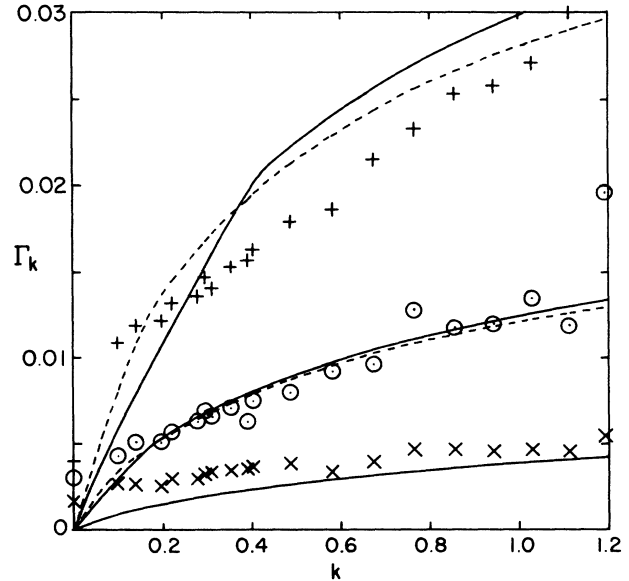


FIG. 1. The damping rate Γ_k for the CLRM is plotted at three different temperatures as a function of wave vector k (k is in units of one over the lattice spacing a). The points represent the simulations (+: $T=0.395$; o: $T=0.289$; x: $T=0.179$) and the curves are given by Eqs. (5.11) and (5.13) where the temperature renormalization of the spin stiffness and the spin-wave velocity have been taken into account. The two curves correspond to different values of the correction parameters u_A and $u_{B_{cl}}$. The dashed line corresponds to $u_A=0$, $u_{B_{cl}}=-0.9$ and the solid line to $u_A=-1$, $u_{B_{cl}}=-1$. At the lowest temperature, the two lines fall on top of each other and at the intermediate temperature they are barely distinguishable. In these units the spin-wave velocity is approximately equal to 1; and the spectrum is roughly linear. Thus, at $k=1$ and $T=0.289$, the ratio of the spin-wave frequency to the spin-wave width is approximately 100. We have not made an attempt to find the best set of fitting parameters u_A and $u_{B_{cl}}$, but simply give reasonable ones that show a qualitatively good agreement.

the widths as a function of k for three different temperatures and two sets of parameters u_A and $u_{B_{cl}}$. The agreement is qualitatively good with both sets and would still be good up to the higher temperature ($T=0.589$) which we have omitted for clarity. In particular, the temperature dependence of the damping in this region comes from the cumulative effects of the T^2 term and the softening of ρ_S . Without the thermal renormalization of ρ_S , the temperature dependence predicted would be much too weak.

In Fig. 2, we plot the logarithm of the ratio γ_k/ω_k as a function of $\log(k\xi)$. In the scaling regime (regime A_{cl}), the ratio depends only on $q \equiv k\xi$, as given by Eq. (1.8). As previously stated, we use $\delta=1.7$, which was found to accurately predict the location of the spin-wave peaks.⁵ The two dashed lines correspond to different values of the constant u_A . They are in qualitative agreement with the low-temperature data and deviate strongly from the high-temperature data. This is to be expected, since formula (1.8) is only valid for $\ln(q) \gg 1$. At smaller values

of $\ln(q)$, we compare the data points with a scaling formula that was used in Ref. 5. The scaling form was chosen there to be

$$\Gamma_k/\omega_k = \frac{\gamma_0(1+\mu q^2)^{1/2}}{\left[1 + \frac{\theta}{2}\ln(1+q^2)\right]^{3/2}} \times \frac{1}{\sqrt{3/2}q[\delta + \frac{1}{2}\ln(1+q^2)]^{1/2}}, \quad (6.10)$$

with three adjustable parameters. In THC, the parameters were determined by a fit of the whole dynamical correlation function; it was not a direct fit of Eq. (6.10) to the Lorentzian linewidths. The best parameters for the overall fit were

$$\gamma_0=0.8, \quad \mu=2.0, \quad \theta=0.15. \quad (6.11)$$

The solid line represents Eq. (6.10). One sees in Fig. 2 that the data points at high temperature obey scaling very well; indeed, the points corresponding to different temperatures but the same value of q fall on top of each other. In order to find the right scaling formula, one

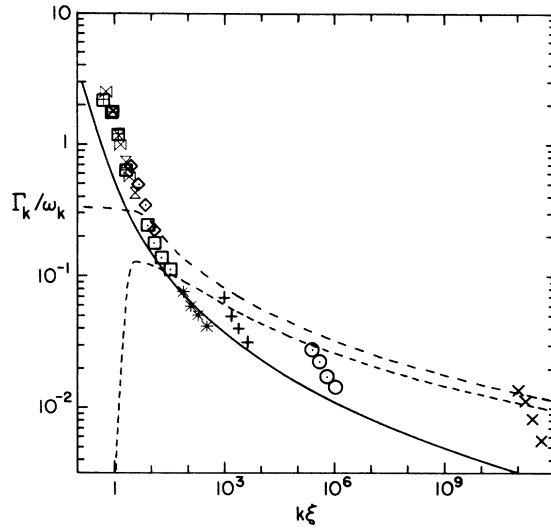


FIG. 2. The ratio of the damping to the spin-wave frequency is plotted as a function of the scaling variable $q \equiv k\xi$, where k is the wave vector and ξ the correlation length. The data points correspond to nine temperatures: \boxplus , $T=0.889$, $\xi \approx 2.6$; \boxminus , $T=0.845$, $\xi \approx 3.0$; \boxtimes , $T=0.773$, $\xi \approx 4.3$; \diamond , $T=0.654$, $\xi \approx 14$; \square , $T=0.589$, $\xi \approx 38$; $*$, $T=0.478$, $\xi \approx 370$; $+$, $T=0.395$, $\xi \approx 4900$; \circ , $T=0.289$, $\xi \approx 1.2 \times 10^6$; \times , $T=0.179$, $\xi \approx 5.0 \times 10^{11}$. At each temperature four data points are shown corresponding to different values of k . At the higher temperatures, the data points scale well, while at the lower temperatures, they are out of the scaling regime (regime A_{cl}). The solid curve is a simple scaling form that was used in a previous paper in the region of high temperatures ($0.6 \lesssim T \lesssim 1$); it is given by Eq. (6.10). The dashed curves represent the low-temperature scaling function derived from the analytic damping calculations of the present paper, as given by Eq. (1.8) for two values of the parameter u_A . The upper dashed curve has $u_A=0$ and the lower $u_A=-1$.

should interpolate between the high-temperature data points and the low-temperature dashed lines.

The fact that the data from the lower temperatures do not fit quantitatively on a single scaling curve is most likely due to a combination of difficulties: The data at short wavelengths are outside of the expected scaling region, while the data at the longest wavelengths may suffer from inaccuracies due to finite-size effects and our limited frequency resolution.

VII. CONCLUSION

In this paper, we have calculated the damping of spin waves in the 2D Heisenberg antiferromagnet at low temperatures and long wavelengths. The primary conclusion is that, in all regimes, as long as $k\xi \gg 1$, where k is the wave vector and ξ is the correlation length, the spin waves are well-defined excitations. They are well defined in the sense that, for any finite positive x , if $k \rightarrow 0$ and $T \rightarrow 0$ with $ka \propto (T/\rho_S)^x$, then the ratio of the spin-wave width to the spin-wave frequency tends to zero ($\gamma_k/\omega_k \rightarrow 0$).

This is different, however, from the situation in three dimensions. In three dimensions, hydrodynamics predicts that the magnons are well defined in a stronger sense: At any finite temperature ($T < T_{N\acute{e}el}$), in the limit of long wavelengths ($k \rightarrow 0$), the ratio of the spin-wave width to the spin-wave velocity tends to zero ($\gamma_k/\omega_k \rightarrow 0$). Indeed, regardless of dimension, the prediction of hydrodynamics for the damping rate is¹⁹

$$\Gamma_k = Dk^2. \quad (7.1)$$

But the hydrodynamic damping is given by the short-wavelength fluctuations and neglects completely the damping due to the interaction of long-wavelength magnons. It is a good approximation in high dimensions where the phase space available for these processes is small ($\propto k^{d-1}dk$), but as one lowers the dimension d , one reaches a point where the long-wavelength modes become dominant: This is the case in two dimensions according to our calculation.

It is interesting to remark that, in the similar calculation in three dimensions, the damping was always dominated by thermal magnons ($p \sim \tau$).⁶ This validates the assumption of hydrodynamics in three dimensions (the dominant damping occurs at comparatively short wavelengths). By contrast, in two dimensions at long wavelengths, the damping is dominated by the momenta p in the interval $k < p < k/T^2$, which cannot be treated by hydrodynamics. Another difference between the calculation in three dimensions and in two dimensions, is that, in three dimensions, the curvature of the spectrum sets the crossover between regimes A and B , while, in two dimensions, the crossover is given by the condition of self-consistency.

In sum, we have calculated the damping of spin waves in four different quantum regimes and two classical regimes. When properly renormalized, our quantum results should be valid for any finite S , in the limit of low temperatures and long wavelengths. We have given a scaling form for the damping valid in the region where

$1 \ll k\xi < \infty$ which applies identically to the quantum and classical scaling regimes. We have performed simulations of the classical lattice rotor model to test the results for the damping in different temperature ranges. At low temperatures ($T < 0.6$), we have found that the dependence of the damping on temperature and wave vector was qualitatively well predicted by the calculations when we include the renormalization of the parameters due to thermal fluctuations. This is an important consistency check of our results.

We must note that our results are in contradiction with a recent publication by Becher and Reiter²⁰ where they obtained a damping rate for spin waves in the 2D QHAF that is proportional to k^2 and independent of temperature, in the limit $T \rightarrow 0$ for fixed small k . Reiter has also suggested²¹ that the spin-wave damping rate is proportional to T^2 , and independent of k , in the limit where $k \rightarrow 0$ more rapidly than T , but $k \gg \xi^{-1}$, which disagrees with our own calculations in both the classical- and quantum-mechanical cases. A more recent analysis by Becher and Reiter has revealed an error in the previous work, however, and they conclude that at least to order $1/S$, the damping of spin waves does vanish at $T=0$, for small values of k , and there is no damping of order T^2 at finite temperatures for $k=0$, in agreement with our results. In fact, we believe that the magnons should have zero damping in this limit, as long as the zero-temperature magnon spectrum has a negative curvature at small k . If the spin-wave expansion converges, the curvature must be negative at least for large values of S , and most likely even for $S = \frac{1}{2}$.

We are also in contradiction with Grepel,²² who has calculated the damping in the limit $\hbar\omega > T$ (corresponding to either regime *C* or regime *D*). Grepel finds in this limit that

$$\Gamma_k \approx c\xi^{-1}, \quad (7.2)$$

which is considerably smaller than our results for either

regime. However, Grepel states that he is neglecting the effect of long-wavelength magnon scattering, which probably accounts for the discrepancy.

In 1986, Kosevich and Chubukov²³ calculated the fluctuation corrections to the frequency spectrum of a 2D Heisenberg antiferromagnet using the Dyson-Maleev formalism. They quote an estimate for the damping in the long-wavelength regime, $\Gamma_k \sim \varepsilon_k T$, which differs from our results of regimes *A* and *B* by a multiplicative logarithmic correction. They do not give a derivation of their results, however.

Our formula (1.4) for the damping in regime *D* of the quantum-mechanical case is in agreement with the results of Kopietz,²⁴ who has independently calculated the magnon damping of the 2D quantum antiferromagnet at short wavelengths, including ka of order unity. We are grateful to Kopietz for pointing out an omission of a factor of 2 in the formula for regime *D*, which appeared in an earlier version of our paper.

Wysin, Bishop, and Gouvea²⁵ have reported simulations of a two-dimensional classical Heisenberg antiferromagnet wherein the damping of spin waves was obtained. Results of these calculations have not yet been published, however, and we are at present unable to make a comparison with our analytic formulas or our own simulations of the CLRM.

ACKNOWLEDGMENTS

The authors are grateful for helpful conversations with S. Chakravarty, P. C. Hohenberg, D. Nelson, and R. Morf. We are grateful to B. Rosenstein for pointing out to us the relevance of the papers cited as Ref. 16. One of us, S.T., would like to thank M. Szabó for encouragement. This work was supported in part by the National Science Foundation (NSF) through Grant No. DMR 88-17291, and the Harvard Materials Research Laboratory. Computations were performed on a Cyber 205 at the John von Neumann Computer Center.

*Present address: Laboratoire Central de Recherches, Thomson-CSF, 91404 Orsay CEDEX, France.

¹S. Chakravarty, B. Halperin, and D. Nelson, *Phys. Rev. B* **39**, 2344 (1989).

²Y. Endoh, K. Yamada, R. J. Birgeneau, D. R. Gabbe, H. P. Janssen, M. A. Kastner, C. J. Peters, P. J. Picone, T. R. Thurston, J. M. Tranquada, G. Shirane, Y. Hidaka, M. Oda, Y. Enomoto, M. Susuki, and T. Murakami, *Phys. Rev. B* **37**, 7443 (1988).

³K. Yamada, K. Kakurai, Y. Endoh, T. R. Thurston, M. A. Kastner, R. J. Birgeneau, G. Shirane, Y. Hidaka, and T. Murakami, *Phys. Rev. B* **40**, 4557 (1989).

⁴G. Aeppli, S. M. Hayden, H. A. Mook, Z. Fisk, S.-W. Cheong, D. Rytz, J. P. Remeika, G. P. Espinosa, and A. S. Cooper, *Phys. Rev. Lett.* **62**, 2052 (1989).

⁵Stéphane Tyč, Bertrand I. Halperin, and Sudip Chakravarty, *Phys. Rev. Lett.* **62**, 835 (1989).

⁶A. B. Harris, D. Kumar, B. I. Halperin, and P. C. Hohenberg, *Phys. Rev. B* **3**, 961 (1971).

⁷P. C. Hohenberg, *Phys. Rev.* **158**, 383 (1967); N. D. Mermin and H. Wagner, *Phys. Rev. Lett.* **17**, 1133 (1966).

⁸I. Affleck, T. Kennedy, E. H. Lieb, and H. Tasaki, *Commun. Math. Phys.* **115**, 477 (1988).

⁹J. D. Reger and A. P. Young, *Phys. Rev. B* **37**, 5978 (1988); D. A. Huse, *ibid.* **37**, 2380 (1988); D. A. Huse and V. Elser, *Phys. Rev. Lett.* **60**, 2531 (1988); M. Gross, E. Sanchez-Velasco, and E. D. Siggia, *Phys. Rev. B* **39**, 2484 (1989); T. Kennedy, E. H. Lieb, and B. S. Shastry, *J. Stat. Phys.* **53**, 1019 (1988).

¹⁰F. J. Dyson, *Phys. Rev.* **102**, 1217 (1956); **102**, 1230 (1956); S. V. Maleev, *Zh. Eksp. Teor. Fiz.* **33**, 1010 (1957) [*Sov. Phys.—JETP* **6**, 776 (1958)].

¹¹T. Holstein and H. Primakoff, *Phys. Rev.* **58**, 1098 (1940).

¹²For a calculation of these quantities in a spin-wave expansion, see T. Oguchi, *Phys. Rev.* **117**, 117 (1960); more recent estimates can be found in R. R. P. Singh, *Phys. Rev. B* **39**, 9760 (1989), and in M. Gross, E. Sanchez-Velasco, and E. Siggia, *Phys. Rev. B* **40**, 11328 (1989); N. Trivedi and D. Ceperly,

- Phys. Rev. B **37**, 2353 (1989).
- ¹³F. G. Dyson, Phys. Rev. **102**, 1217 (1956); **102**, 1230 (1956).
- ¹⁴G. Parisi, Phys. Lett. **92B**, 133 (1980).
- ¹⁵S. H. Shenker and J. Tobochnik, Phys. Rev. B **22**, 4462 (1980).
See also M. Fukugita and Y. Oyanagi, Phys. Rev. Lett. **123B**, 71 (1983) and S. Itoh, Y. Iwasaki, and T. Yoshié, Nucl. Phys. **B250**, 312 (1985).
- ¹⁶The identity of the interactions among the Goldstone bosons of a lattice rotator model (or nonlinear σ model) and the Heisenberg antiferromagnet is actually an example of the "low-energy pion theorems" that are well known in particle physics. See, for example, S. Weinberg, Phys. Rev. Lett. **17**, 616 (1966); C. G. Callou, S. Coleman, J. Wess, and B. Zumino, Phys. Rev. **177**, 2247 (1969); B. Rosenstein and B. J. Warr (unpublished).
- ¹⁷See also, D. S. Fisher, Phys. Rev. B **39**, 11 783 (1989); I. Affleck, Nucl. Phys. **B257**, 397 (1985); F. D. M. Haldane, Phys. Lett. **93A**, 464 (1983); Phys. Rev. Lett. **50**, 1153 (1983).
- ¹⁸R. Morf and E. Stoll, in *Numerical Analysis*, edited by J. Descloux and J. Marti (Birkhäuser, Basel, 1977), see also T. Schneider and E. Stoll, Phys. Rev. B **17**, 1302 (1978).
- ¹⁹B. I. Halperin and P. C. Hohenberg, Phys. Rev. **188**, 898 (1969).
- ²⁰T. Becher and G. Reiter, Phys. Rev. Lett. **63**, 1004 (1989); **64**, 109(E) (1990).
- ²¹G. Reiter, in *Proceedings of Nato Advanced Research Workshop on Interacting Electrons in Reduced Dimensions*, Torino, 1988, edited by D. Campbell (Plenum, New York, to be published).
- ²²D. R. Grempel, in *New Trends in Magnetism*, edited by M. D. Costinho-Filho and S. M. Rezende (World Scientific, Singapore, 1990), p. 133.
- ²³Yu. A. Kosevich and A. V. Chubukov, Zh. Eksp. Teor. Fiz. **91**, 1105 (1986) [Sov. Phys.—JETP **64**, 654 (1987)].
- ²⁴P. Kopietz, Phys. Rev. B **40**, 4846 (1990).
- ²⁵G. Wysin, A. Bishop, and M. Gouvea, Bull. Am. Phys. Soc. **34**, 847 (1988).